

Authors' response to interactive comment of the Referee #1

Black text: Referee comment

Blue text: Authors' response

We thank the reviewer for the valuable comments and suggestions to improve our contribution. We provide point-by-point reply below.

Abstract: there were several models mentioned in the abstract, which makes readers confusing for the first impression. To make it clear, I suggest to use the name that the author described in section 2.3.5: HILLFLOW–Couvreur–SLIMROOT–LINTULCC2 for the newly coupled model and HILLFLOW–Feddes–SLIMROOT–LINTULCC2 for the commonly approach at line 18

10 The name of the coupled model has changed in the abstract that it is consistent with section 2.3.5.

Introduction: The author wanted to simulate the water and gas fluxes for different water and soil conditions considering dynamic plant hydraulics. The importance of dynamic plant hydraulics was well presented. Dynamic plant hydraulics related to root growth so root development was needed. The author used SLIMROOT but did not mention and explain why it was chosen in the introduction.

15 The coupling root-shoot model required a use of root growth model. For a valid comparison, it is necessary to couple both RWU models and water balance model with the same root growth model. From this point, the root growth model with a dynamic root growth (over time and soil layers) was chosen to inform the root depth, root length, and root length density (or normalized root length density) for Feddes and Couvreur RWU approach. Thus, the authors thought that it might not be necessary to mention and answer why SLIMROOT was employed right away from the Introduction section. However, the SLIMROOT root growth model was described in detail in the section 2.3.2.

Methods and Materials:

This manuscript described five different models and each of them has different parameters (input and output). It's good that all the parameters and related values were listed in the supplementary materials. These five models were coupled in two different ways and the input or output of the models were used from each other. I suggest the author draw a diagram or flowchart to describe the connection between the models, which will definitely help readers to understand better.

25 The modelling couple was the same for both RWU approaches. The coupling configuration namely linkages of shoot growth, root growth, water balance, and root water uptake model was the identical to ensure the analysis and comparison of two different RWU models. As suggestion of referee's comments, a diagram was added (see Figure 2). A short paragraph was added to explain the Figure 2.

30 "For a certain hourly time step $\Delta t_i = t_i - t_{i-1}$, different modules were solved in the following sequence. First, LINTULCC2 was used with a water stress factor $f_{wat} = 1$ to calculate the leaf and canopy resistance, and the potential transpiration rate. T_{pot} was then used in HILLFLOW 1D to calculate the soil water pressure head changes, water content changes, the actual transpiration, and f_{wat} during the time step. LINTULCC2 was then run again using the f_{wat} . The leaf conductance and assimilation rate were calculated. For the next time step, the same loop was run and hourly assimilation was accumulated to a daily value. Daily assimilation rates were used in modules that run with a daily time step. For instance, modules of LINTLCC2 that calculate assimilate partitioning which is used to calculate shoot (LAI) development and passed to SLIMROOT to simulate root development (Fig. 2)."

40 For the root growth model, soil water content and soil temperature were needed for the simulations. It seems that the author used simulated results from two separate models. Why did not the authors use the measured data from the soil sensors for the root growth simulations?

The authors can use directly the measured root growth which was collected weekly by minirhizotubes for the daily simulation by assuming that root growth will not change much within one week (as similar to the work from Cai et al., 2017; Cai et al., 2018). In addition, the measured soil water content and soil temperature can be use as the “forced input” for the root growth simulation. We used the “forward modelling approach” which weather data, soil, and crop parameters are the input for two coupled models. Soil water content is simulated by water balance model HILLFLOW 1D. The soil temperature is calculated by the subroutine in the root growth model (STMPsim, Williams and Izaurrable, 2006) (see the new diagram Figure 2). The output data (i.e the performance of root growth simulation) was evaluated directly with the observed root data, while the simulated soil water content was compared with the measured soil water content data.

Stomatal conductance (g_s) could also be used for explaining the variation of the transpiration, especially for dry conditions. The reduction in g_s shows water stress. Since these data were available (Appendix A) the variation of g_s and f_{wat} could be related somehow. The author could show and discuss it in the results and discussion part.

The leaf water potential is surrogate of stomatal regulation our study. By showing simulated leaf water potential, transpiration, and gross assimilation rate in comparison to the measure data (Fig. 8), our work has showed that the model is able to simulate water stress effects on leaf water potential and gas exchange in different measured days (for instance Couvreur model). As suggested by the referee, the simulated stomatal conductance to water vapor (here from sunlit leaves) was compared with the measurement from 3-4 upmost fully developed leaves. Two sentences were added to describe the measurement of leaf gas exchange together with leaf water potential and one sentence was added for the simulation results of stomatal conductance in comparison with the measured ones.

Results and discussion: line 479 and this paragraph were a little bit off, especially the comparison between the modern and old cultivars. This part could be either skipped or connected with a better explanation.

This paragraph was removed and improved (see also reply to the comments with sensitivity analysis section from referee # 2)

Conclusion: the aim of the study, drawback of the models, and further investigations were well presented. The three objectives of the study were posted at the end of the introduction and they were tested in the manuscript but not all of them were mentioned in the conclusion part. Normally, answers should be given in the end.

The Conclusion part was revised (together with comments from referee #2)

Line 10: the sentence is really long, please rephrase.

This was rephrased and shortened down.

Line 22: LAI is not defined before, please give the full name, leaf area index

It was given full name.

Line 30: ‘promissing’ – ‘promising’

It was corrected.

Line 39: move (RWU) to the former 'root water uptake'. Please also check the usage of 'RWU' and
80 'root water uptake' in the text below. Once it is described, the abbreviation should be used
afterwards.

It was moved.

Line 47: 'in an indirect manner' – 'indirectly'

It was corrected.

85 Line 50: 'models of root water uptake' – 'RWU models'

It was corrected.

Line 65: delete 'shoot'

It was deleted.

Line 86: missing the 'period' symbol

90 It was added.

Line 106: delete 'soil property' since the soils have been described before

It was deleted.

Line 110: 'side' – 'sides'

It was corrected.

95 Line 112: 'was' – 'were'

It was corrected.

Line 115: 'rain-fed' – 'rainfed' and also check it in the text below

It was corrected and made consistently for the next paragraphs.

Line 119: ... sap flow was calculated ...

100 It was corrected.

Line 123: '8pm' – '8 pm'

It was corrected.

Line 130 and 131: '6' – 'six'

It was corrected.

105 Line 132: use am (pm) or AM (PM) in the whole text

These will be made consistently in the whole text.

Line 150: 'above ground' – 'aboveground', and also check it in the text below

These will be changed consistently in the whole text.

Line 151: the detailed measurements of biomass, especially the different organs, were described but not used later.

110 This part could be skipped

It was kept like this because the separated organs need to be measured then the total aboveground biomass is determined from the sum of different organs.

Line 162: ... model of Farquhar and Caemmer (1982)

It was corrected.

115 Line 165: For the sake of ...

It was corrected.

Line 167: check the format of the citations in the bracket

It was corrected with the right citation format.

Line 171: give the full name of LAI
120 The full name of LAI was added
Line 190: keep 'Hillflow1D' and 'HILLFLOW 1D' the same in the text
It was corrected and made consistently in the text.
Line 229: 'fwat' – 'fwat' and also in Figure 4
It was corrected.

125 Line 323-324: Not clear. It is better to have two different colors or symbols to differentiate the two samples.
These were two replications of biomass and LAI. It was rewritten for better understanding.
Line 325: do you use the mean r^2 of the six plots? If so, you need to mention and also re-calculate them. It seems that 0.91 and other values are not the mean of the six values.

130 The r^2 , RMSE, and I were calculated when all measurements from 06 plots were pulled together (they are not the mean of six values from six plots).
Line 343: use 'minirhizotube' or 'rhizotube' in the text and in the caption of the figures
The minirhizotube will be used and changed consistently in the text and the figure captions.
Line 363: ... show the simulated ..., by the ...' – '... show ..., simulated by ...'
135 It was revised.

Line 407: 'Pg' is not defined
Pg will be defined in the text.
Line 463: 'increases' – 'increase'
It was corrected

140 Line 477: 'is' – 'are' Figure 2,
It was corrected.
Line 879: 'green' – 'cyan' (used in Figure 2 and 4) Figure 4: make the size of the four subplots (a, b, c, d) the same for better comparison Figure 4,
It was corrected. The size of the subplots will be similar in Figure 4.

145 line 934: Pg? Please give the full name
The full name was added.
Appendix F: bar plot will be better for the comparison
The plot was converted to bar plot.

150

155

160 **Authors' response to interactive comment of the anonymous Referee #2**

Black text: Referee comment

Blue text: Authors' response

We thank the reviewer for the valuable comments and suggestions to improve our contribution. We provide point-by-point reply below.

165 **General Comments**

This study compares two crop and root growth models with measured data that were previously published. The models differ mainly in their representation of root water uptake. One uses the standard approach (Feddes), the other considers the flow process in the roots (but not to the roots) and is hence more mechanistic. The paper is fairly well written. It is a valuable contribution to soil/crop science, but would benefit from a few extensions and corrections, as outlined below.

170 Thank you for your comments. The measured data has not published before. However, the soil parameters and RWU parameters from two RWU models were published in the previous studies (with the same experimental set-up but in 2014). The published the soil parameters and RWU parameters from two RWU models were used in this study.

175 It is a severe shortcoming of the measurements that the field plots do not involve replications. Replicates would be very desirable to enable assessing the variability, but their omission should not prevent the manuscript from being published. It should be frankly stated that and why there were no replicates (too expensive?). The experiment should be described better (e.g., the plot size is not given).

Yes. We agreed that the field plots did not involve replications.

180 The construction and experimental designs were described in detail in Cai et al., (2016); Cai et al., (2017) and Cai et al., (2018). The authors also referred the readers for the detail explanation of field trial these papers. As suggested from the referee, we added one sentences in the section 2.1 (Location and experimental set-up) between line 95 and 97.

“Each treatment was 3.25 m wide and 7 m long. The treatments bordered each other along 7-m-long side”.

185 One paragraph was added to discuss the limitation of experimental set-up in the result and discussion section (Line 482)

In model-measurement comparisons, it is good practice to present the measured data with standard deviations or errors and the modeled data as lines; if uncertainty is considered, with uncertainty bands. This is not always the case here (Figure 3 no, figure 4 yes; why?)

190 Figure 4 showed the transpiration by two models versus the measured sap flow. The measured sap flow was achieved with 5 sensors in each plot. Thus, the variability of transpiration from different stems could be shown via error bars. The Figure 3 showed the simulated root length density versus the observed root length in 06 soil depths in different treatments. For one observation depth and one treatment, roots were counted in 120 images of 13.5 mm x 18 mm. This dataset represents a sample of the population of all possible root counts at this depth. Cai et al.,
195 (2016) estimated and analyzed the standard deviation (error) and spatial correlation of root counts along the minirhizotube. The standard deviation was small and no spatial correlation of root densities in the horizontal direction was observed for the investigated **winter wheat** crop. That is a reason that Figure 3 we did not show the standard deviation for the root measurements.

200 The paper should give a few more details about the calibration of the soil-crop model. The role of Penman's ETP should be discussed.

The calibration was mentioned in line 296-302. Following the suggestion from the referee, the calibration sentences was revised and is added more details.

205 "Before comparing these modelling approaches, we calibrated the original LINTULCC model using the data from the rainfed plots in the silty soil (F2P2). The model is firstly calibrated to make sure the model properly described the phenology. Two parameters (minimum thermal sum from sowing to anthesis and thermal sum from anthesis to maturity ($^{\circ}\text{C d}$)) were used for phenology calibration based on information of sowing, anthesis, and maturity dates. The model was then calibrated using time series of LAI, biomass, and gross assimilation rate through the change of maximum carboxylation rate at 25 $^{\circ}\text{C}$ (VCMAX25), critical leaf area index (LAICR), and relative growth rate of leaf area during exponential growth (RGRL) parameters."

210 Regarding the potential evapotranspiration (ETP), our study used the Penman-Monteith equation from Allen et al., (1998) (See Equation 3, Chapter 2 in the FAO Irrigation and Drainage Paper No. 56, Allen et al., 1998). The ETP was calculated with crop canopy resistance under optimal water condition ($f_{\text{wat}} = 1$) (see the Appendix B). The hourly net radiation, soil heat flux, and aerodynamic resistance were estimated based on Allen et al., (1998) (see also the replies for comments at line 559, 561, and 565). Following suggestion from the referee, some sentences

215 were added after line 429 to describe the roles of ETP.

"The method that we used for modelling the canopy resistance used in the Penman-Monteith has been reported for both short and tall crops (Dickinson et al., 1991; Kelliher et al., 1995; Irmak & Mutiibwa, 2010; Perez et al., 2006; Katerji et al., 2011; Srivastava et al., 2018). The fair agreement of RWU to sap flow in our study indicates the proper estimate of ETP based on the crop canopy resistance (with $f_{\text{wat}} = 1$) in winter wheat. The direct calculation

220 of crop canopy resistance in our work allows to capture physiological responses of the crop (stomatal conductance) to solar radiation, temperature, and vapor pressure deficit (Eqn. A5). In addition, this approach also avoids calculating grass reference evapotranspiration based on a constant canopy resistance."

The Conclusion section should be improved. The first paragraph is misplaced. I would like to hear a bit more about the rhizosphere conductivity under drought and see the work (at least one paper) of Andrea Carminati cited in this

225 context. Model testing is important but how could the model be improved? Is it not a severe shortcoming that the drop in root length density in the topsoil is neglected? And, similarly, the increased root growth under drought stress? How could this be represented better in the model? What models are already out there that are capable of handling such situations?

The conclusion section was revised which should answer the mentioned objectives in the Introduction (see

230 comments from Referee # 1) and will be added some suggestions from Referee #2. The first paragraph is shortened down to conclude for the first objective. The second graph concluded the model ability in simulating plant hydraulic conductance (which is for the second objective) with more insights of rhizosphere conductance and citation from Andrea Carminati. The third paragraph concluded for the results from sensitivity analysis (third objective). The last three small paragraphs mentioned on the model limitations and outlooks. Some root growth modelling approaches

235 will be added that we can lean and improve the models.

"We evaluated two different root water uptake models of a coupled soil water balance and crop growth model. One root water uptake model was the often used Feddes model whereas the other, the Couvreur RWU model represents a "mechanistic" RWU that explicitly simulates the continuum in water potential from soil to root, and

240 to leaf based on the whole plant hydraulic conductance. Overall, the measured biomass growth, LAI development, soil water contents, leaf water pressure heads, and transpiration rates were well reproduced by both models. But, the Fe model incorrectly predicted more water stress and less growth in the silty soil than in the stony soil whereas the opposite was observed. The Fe model does not account for the higher plant conductance in the silty soil where more roots were simulated than in the stony soil. In addition, the Fe model does not consider root water uptake compensation which reduces water stress. In other words, the Feddes approach did not possess the flexibility as compared to Couvreur model in simulating RWU for different soil and water conditions.

245 Based on the absolute root length, the Co model was able to simulate K_{plant} in different soils and treatments. The simulated K_{plant} followed the root growth and reached a maximum at around anthesis. However, the observed K_{plant} was lower in the sheltered plots although the observed total root lengths in these plots were almost similar (stony soil) or larger (silty soil) as compared to the irrigated and rainfed plots. Moreover, the higher simulated K_{plant} in comparison to the observed values in the sheltered plots suggested that the newly coupled model needs to consider the declined hydraulic conductance of the root-soil interface due to decreased soil water pressure head. The formation of air gaps at soil-root interface due to the root shrinkage of roots and root-soil contact loosening (Carminati et al., 2009) could induce a strong increase of hydraulic resistance to radial water flow between soil and roots.

255 A mechanistic model that is based on plant hydraulics and links root system properties to RWU, water stress, and crop development can evaluate the impact of certain crop properties (change of root segment conductance, specific weights of root, or leaf pressure head thresholds) on crop performance in different environments and soils. The Co model could capture the positive feedbacks between the aboveground biomass, the root length, the total root system hydraulic conductance, and finally K_{plant} .

260 In this study, a higher total root length was simulated in the silty soil than in the stony soil because a higher specific root length was found for root growth in the silty soil. This can be considered as an extra relationship that requires attention in crop modelling. Crop growth models will need to consider soil specific calibration to account for differences in specific root length with soil. Alternatively, a more mechanistic description of root growth that predicts root specific length would reduce the amount of calibration in crop growth models. Another aspect in demand of improvement is the prediction of the root distribution with depth. In our simulations, highest root densities were simulated in the top soil whereas the observations showed higher densities in the deeper soil layers. Examples of detailed 3D root growth models that could improve the simulation of root distribution are given by Dunbabin et al., (2013). The coupling of a shoot model with a 3D root growth model that represents root system architecture simulated more accurate root distributions (at both top and subsoil layers) under drought conditions (Mboh et al., 2019). Nevertheless, simulating the third dimension of root growth would largely extend the parameter requirements which makes them more difficult for testing under the field.

275 Finally, the model did not consider changes in carbon allocation to the root system that are triggered by stress. Therefore, the model simulated less roots in the water stressed sheltered plot of the silty soil whereas more roots were observed in this plot compared with the other plots in this soil. A more mechanistic description of root: shoot partitioning of both carbon and nitrogen (Yin & Schapendonk, 2004) or carbon allocation as a function of soil water conditions (i.e. soil water potential in Kage et al., (2004) and Li et al., (1994)) would be needed to refine the prediction of responses of root development to water stress.

280 Future research should focus on testing the newly coupled model (HILLFLOW–Couvreur’s RWU–SLIMROOT–
LINTULCC2) for other wheat genotypes and crop types (isohydric like maize) and for a wider range of soil and
climate conditions. Further improvements should particularly be targeted leaf area simulation. Improving the
modelling of leaf growth should result in better simulations of LAI and more accurate estimates of energy fluxes
at canopy level.”

285 Does the fact that P1 receives less water but is exposed to the same weather situation in regard to all other weather
variables (e.g., air humidity) as P2-P3 might have biased (in the sense of an artifact) the reaction of crops in the
field as compared to the simulations?

290 We agreed and understood that in the field, the rainout shelters might influence the P1 itself and nearby P2 and P3
plots with regard to air circulation (and thus air humidity and canopy temperature). We also expected that there
could be a difference with regards to microclimate conditions and crop reactions amongst the plots. We tried to
minimize as much as possible the effects of shelter application on climatic conditions and crop growth. The rainout
shelter was used when it rains and removed directly when rain stops to minimize the effects of the shelter within
the plot P1 and on plot P2 and P3. Water was collected by the shelter from P1 was drained out that did not pour on
the P2.

Detailed comments

line 41 function of

295 It was corrected

44 correct: are lost

It was corrected

300 46 make clear that you use the terms water potential and hydraulic potential coherently. Better, define it for the
readers from different fields. There is a problem because traditionally for plant scientists water potential does not
contain the gravitational component, for soil scientists it does. What is root zone water potential? Is it the hydraulic
or matric potential in the rhizosphere? probably not.

It was corrected. One sentence (see line 46) was added to clarify the terms in the introduction part and used
consistently for the whole paper.

58 computation of

305 It was corrected

228 In both models, delete "for each model"

It was corrected

235, 240 in a given layer

It was corrected

310 238 delete "sufficient"

It was changed

239 I recommend deleting "which is based on a mechanistic description of water flow in the coupled soil-plant
system," because you are her in the technical part.

It was deleted

315 252 delete "the"

It was deleted

287 UTC is more confusing than local time

We do not understand clearly this comment. It is important to match time of weather input data and output data from the models with the time of the measured data. The conversion of the local time (CEST and CET in Germany) to UTC time aims at avoiding the time confusion since the UTC is standard time which might help the paper targets to “broader readers”.

320
292 better "characterizes the difference" or "is a measure for the difference"
It was changed “characterizes the difference”.

297 "are uncertain"
It was changed.

325
304 seminal roots
The range of value is for the lateral root. This will not be changed.

310 units missing
Unit was added.

330
311 threshold (index)
We agree, threshold was added.

316 better reverse: kplant explicitly simulated by...
This was changed.

317 we present and discuss the results of the sensitivity analysis
It was revised.

335
324 in fair agreement (at best)
It was revised.

358 Grammar: this should not be emphasized too much Content: This cannot be emphasized too much because it shows a clear and important shortcoming of your modeling approach and gives a point of leverage for the next step of improvement.

340
It was revised.

366 better: transpiration rates simulated by the Fe/Co model or simply transpiration rates by the Fe/Co model
It was revised.

376 less dry
It was revised.

345
379 "from" end of May

404 I do not understand how you define adequate. I would rather write fair.
It was revised.

407 Pg is not defined. For the reader, it is better to write it out.

350
Thank you. The Pg is defined.

443 the sheltered plot with the silty soil (the field is the same - according to figure 1) if this is not true add the field borders in figure 1
This is in line 433 not line 443. The two sites were in the same field (around 200 m long). There is no field borders however the two sites were situated in two different soil types. The text was revised.

355
444 comma before based
It was revised.

445 delete "in the measurements" (perhaps: observed in the field)

It was revised.

446 and elsewhere see above 443

360 It was revised.

450 must have causes not considered in the model (“other causes that“ is wrong here)

It was revised.

455 The sensitivity analysis is, frankly speaking, a bit boring (sorry). It destroys the flow of the paper and feels like a "lost part". The reader should be left off the hook after Figure 9, but (recommendation) after a better discussion of what he or she can learn from all that.

365

Thank you very much for your suggestion. The couple root: shoot model with such the mechanistic RWU Couvreur model with considering two ways coupling has not been done before. This is the first study to evaluate the performance of the coupled root: shoot model. Thus, the sensitivity analysis is strongly necessary because of several reasons (i) to understand the roles of important parameters of Courvreur model itself (critical leaf water pressure head and plant hydraulic conductance) and other root hydraulic conductance parameters which are rarely available at field scale (see Cai et al. 2017 and Cai et al., 2018) or the root parameters which are often used in crop models that might contribute to plant hydraulic conductance (ii) to understand the feedbacks and effects of aboveground biomass, root growth, root system hydraulic conductance, whole plant hydraulic conductance, and leaf water pressure head threshold on RWU and biomass (iii) the feedbacks of aboveground crop growth to belowground can be only analyzed with Courvreur model (iv) by doing this analysis, the important roles of hydraulic conductance and necessity of two-ways couple can be emphasized. Thus, the authors would like to keep this section (together with Fig.10). However, the section is shortened down. Line 479 to lines 487 will be deleted (see also the replies to comments from Referee #1 on this paragraph).

370

375

479 are lower than those of old cultivars (not were)

380

It was revised.

481 indicates that

It was revised.

490 potential

It was revised.

385 495 more mechanistic, then you can drop the quotation marks

It was revised.

496 no comma

This in line 499. It was revised.

549 How were x_j and w_j determined? Should it not read $LAI(x_j)$?

390

The formulation was revised by adding the multiplicative symbols. The approach for upscaling from leaf to canopy was described in Goudriaan & van Laar (1994). Further mathematical information can be found in Stoer and Bulirsch (2002). The estimate of x_j and w_j can be derived from page 178, Chapter 3.6. “Gaussian Integration methods”. An integral from $[0, LAI]$ needs to be changed into integral over $[-1, 1]$ before using the Gauss–Legendre quadrature. The x_j and w_j can also be found from https://en.wikipedia.org/wiki/Gaussian_quadrature.

395

554 "thus there was no Gaussian integration over time degree“ - this cannot be understood

It was revised

559 better write "grass reference evapotranspiration (FAO, give the reference)“

Please see our above reply for the role of ETP calculation with Penman-Monteith equation. This is not grass reference evapotranspiration. The potential evapotranspiration (ETP) is calculated by hourly Penman-Monteith equation from Allen et al., (1998) (See Equation 3, Chapter 2 in the FAO Irrigation and Drainage Paper No. 56, Allen et al., 1998). The ETP is calculated from non-stress crop canopy conductance ($f_{wat} = 1$, see Figure 2).

561 reference needed

Reference was added

565 How were surface resistance and aerodynamic resistance calculated?

The “surface resistance” was corrected. The surface resistance is crop canopy resistance (Eqn. B5). The hourly aerodynamic resistance (r_a) is calculated as Equation 4, Chapter 2 in the FAO Irrigation and Drainage Paper No. 56, Allen et al., (1998).

578 verb missing matrix potential, not matrix potential matric potential head should have a unit, here m Please make clear in the whole paper if you talk about the soil matric potential or soil hydraulic potential. Otherwise it is confusing. Here, for example, I feel that you mean soil matric potential. Actually I would avoid using the expression soil water potential.

This term was changed in the paper.

Figures

All figure captions should be formulated more carefully and with more empathy for the reader.

The captions were revised.

Figure 1 Indicate what kind of rock.

The rock type was indicated.

Figure 7 You should try to explain the systematic deviation in the deeper soil layers. 998: The should be better described in the text.

The Caption was revised. Thank you for your suggestion. The systematic deviation in the deeper soil layers was explained from Line 444 to 451.

Figure 6, 8 Rephrase the confusing caption. You should start with a statement about what the reader can see. Include the top graphs in the enumeration. Ψ_{leaf} and P_g should be defined in the caption (as RWU).

The caption was revised. The enumeration was added for the top graph. The full names of RWU, P_g , and Ψ_{leaf} were also defined.

Figure 10 should be deleted

This Figure 10 was kept, please kindly see reply Line 455 for the “sensitivity analysis” section

Additional references:

Carminati, A., Vetterlein, D., Weller, U., Vogel, H.-J., & Oswald, S. E. (2009). When Roots Lose Contact. *Vadose Zone Journal*, 8(3), 805–809. <https://doi.org/10.2136/vzj2008.0147>

Dickinson, R. E., Henderson-Sellers, A., Rosenzweig, C., & Sellers, P. J. (1991). Evapotranspiration models with canopy resistance for use in climate models, a review. *Agricultural and Forest Meteorology*, 54(2–4), 373–388. [https://doi.org/10.1016/0168-1923\(91\)90014-H](https://doi.org/10.1016/0168-1923(91)90014-H)

Dunbabin, V. M., Postma, J. A., Schnepf, A., Pagès, L., Javaux, M., Wu, L., Leitner, D., Chen, Y. L., Rengel, Z., & Diggle, A. J. (2013). Modelling root-soil interactions using three-dimensional models of root growth, architecture and function. *Plant and Soil*, 372(1–2), 93–124. <https://doi.org/10.1007/s11104-013-1769-y>

Goudriaan, J., & van Laar, H. H. (1994). Modelling potential crop growth processes. Textbook with exercises. In

Field Code Changed

Formatted: English (United States)

Current issues in production ecology;2 (Vol. 2, Issue 1994).

- 440 Irmak, S., & Mutibwa, D. (2010). On the dynamics of canopy resistance : Generalized linear estimation and
relationships with primary micrometeorological variables. *Water Resources Research*, 46, 1–20.
<https://doi.org/10.1029/2009WR008484>
- Kage, H., Kochler, M., & Stützel, H. (2004). Root growth and dry matter partitioning of cauliflower under drought
stress conditions: Measurement and simulation. *European Journal of Agronomy*, 20(4), 379–394.
[https://doi.org/10.1016/S1161-0301\(03\)00061-3](https://doi.org/10.1016/S1161-0301(03)00061-3)
- 445 Katerji, N., Rana, G., & Fahed, S. (2011). Parameterizing canopy resistance using mechanistic and semi-empirical
estimates of hourly evapotranspiration : critical evaluation for irrigated crops in the Mediterranean.
Hydrological Processes, 129(August 2010), 117–129. <https://doi.org/10.1002/hyp.7829>
- Kelliher, F. M., Leuning, R., Raupach, M. R., & Schulze, E. D. (1995). Maximum conductances for evaporation
from global vegetation types. *Agricultural and Forest Meteorology*, 73(1–2), 1–16.
450 [https://doi.org/10.1016/0168-1923\(94\)02178-M](https://doi.org/10.1016/0168-1923(94)02178-M)
- Li, X., Feng, Y., & Boersma, L. (1994). Partition of photosynthates between shoot and root in spring wheat
(*Triticum aestivu*, L.) as a function of soil water potential and root temperature. *Plant and Soil*, 164, 43–50.
<https://link.springer.com/content/pdf/10.1007/BF00010109.pdf>
- Mboh, C. M., Srivastava, A. K., Gaiser, T., & Ewert, F. (2019). Including root architecture in a crop model improves
455 predictions of spring wheat grain yield and above-ground biomass under water limitations. *Journal of
Agronomy and Crop Science*, 205(2), 109–128. <https://doi.org/10.1111/jac.12306>
- Perez, P. J., Lecina, S., Castellvi, F., Mart, A., & Villalobos, F. J. (2006). A simple parameterization of bulk canopy
resistance from climatic variables for estimating hourly evapotranspiration. *Hydrological Processes*,
532(December 2003), 515–532. <https://doi.org/10.1002/hyp.5919>
- 460 Srivastava, R. K., Panda, R. K., Chakraborty, A., & Halder, D. (2018). Comparison of actual evapotranspiration of
irrigated maize in a sub-humid region using four different canopy resistance based approaches. *Agricultural
Water Management*, 202(February), 156–165. <https://doi.org/10.1016/j.agwat.2018.02.021>
- Yin, X., & Schapendonk, A. H. C. M. (2004). Simulating the partitioning of biomass and nitrogen between roots
and shoot in crop and grass plants. *NJAS - Wageningen Journal of Life Sciences*, 51(4), 407–426.
465 [https://doi.org/10.1016/S1573-5214\(04\)80005-8](https://doi.org/10.1016/S1573-5214(04)80005-8)

470

475

Additional changes

480 **Blue text: Authors' response**

We thank the editor and two reviewers for the valuable comments and suggestions to improve our contribution.

Here are some detail changes in the texts and Tables.

Line 3 and 5: affiliation was updated

Line 166: "LintulCC" – "LINTULCC"

485 Line 197: add "and" after comma

Line 291 and 292: "LintulCC" – "LINTULCC"

Line 327: " $d^{-1}/cm\ cm^{-2}$ " – " $cm\ d^{-1}$ "

Lin 346: "and" was added

Line 348: "under" – "in"

490 "under different" was added

Line 386: the reference was corrected

As suggested from Reviewer #2 and the editor, the discussion of field experiment which did not have replicates was added

Line 492: A paragraph with discussion of having no replicates for plot was added.

495 "The observed field data has been shown and compared with the simulated results from the two models in the in the above-mentioned (3.1.1, 3.1.2, and 3.1.3). The data were collected for both crop growth (root, LAI, and biomass) and gas fluxes at different scales (soil water flux and gas exchange from leaf to canopy) in two contrast soil types and under different water treatments. To our knowledge, this is the unique experimental set-up and dataset for understanding soil-plant processes as well as parameterizing and evaluating of soil-plant-atmospheric models.

500 However, due to complex and costly construction of the underground minirhizotron facilities, there were no replicates for plots in our study. LAI and aboveground biomass showed the large variability not only between water treatments but even in the same plot because of microclimate and soil heterogeneities. The variability of tiller development also considerably influences stem-to-stem variability of sap flow. In addition, the small size of plot did not allow having replicates for manual canopy chamber measurement because it might strongly disturb and alter crop growth, leaf gas exchange, and sap flow measurements of the surrounding areas. Nevertheless, despite of these shortcoming issues, the data illustrated the difference and variability among water regimes in two soil types, and over measured dates that it is still valid for modelling comparison and validation in this study"

505 Line 632: Reference of method and values of x_i and w_j was added.

Appendix C:

510 "VCMAX" – "VCMAX25"

"Soil water potential at anaerobic point" – "Soil water pressure head at anaerobic limit"

"Soil water potential where optimum condition for transpiration" – "Upper limit of pressure head range for optimum transpiration"

515 "Soil water potential for higher transpiration rate" – "Lower limit of pressure head range for optimum transpiration for high transpiration rate, T_{pot3h} "

"Soil water potential for lower transpiration rate" – "Lower limit pressure head range for low transpiration rate, T_{pot3l} "

“Soil water potential at wilting point” – “Soil water pressure head at wilting point”

“Higher transpiration rate” – “High transpiration rate”

520 “d⁻¹/cm cm⁻²” – “cm d⁻¹”

Line 664-670: The terms were also changed to be consistent with Appendix C (see above)

Line 696: Author contribution was added

Figure captions and their order in the text were updated.

Line 1671: “d⁻¹/cm cm⁻²” – “cm d⁻¹”

525

530

535

540

Comparison of root water uptake models in simulating CO₂ and H₂O fluxes and growth of wheat

Thuy Huu Nguyen¹, Matthias Langensiepen¹, Jan Vanderborgh³, Hubert Hüging¹, Cho Miltin

545 ~~Mboh~~¹~~Mboh~~⁴ Frank Ewert^{1, 2}

¹University of Bonn, Institute of Crop Science and Resource Conservation (INRES), Katzenburgweg 5, 53115 Bonn, Germany

²Leibniz Centre for Agricultural Landscape Research (ZALF), Institute of Landscape Systems Analysis, Eberswalder Strasse 84, 15374 Muencheberg, Germany

³Agrosphere, Institute of Bio- and Geosciences (IBG-3), Forschungszentrum Jülich GmbH, 52428, Jülich, Germany

550 ⁴[BASF Digital Farming GmbH, Im Zollhafen 24, 50678 Koeln, Germany](#)

Formatted: English (United States)

Correspondence to: Thuy Huu Nguyen (tngu@uni-bonn.de)

Abstract. Stomatal regulation and whole plant hydraulic signaling affect water fluxes and stress in plants. Land surface models and crop models use a coupled photosynthesis-stomatal conductance modelling approach. ~~Those models and~~ estimate the effect of soil water stress on stomatal conductance directly from soil water content or ~~matrix-soil hydraulic~~ potential without explicit representation of hydraulic signals between the soil and stomata. In order to explicitly represent stomatal regulation by soil water status as a function of the hydraulic signal and its relation to the whole plant hydraulic conductance, we coupled the crop model LINTULCC2 and the root growth model SLIMROOT with Couvreur's root water uptake model (RWU), and the HILLFLOW soil water balance model. Since plant hydraulic conductance depends on the plant development, this model coupling represents a two-way coupling between growth and plant hydraulics. To evaluate the advantage of considering plant hydraulic conductance and hydraulic signaling, we compared the performance of this newly coupled model with another commonly used approach that relates root water uptake and plant stress directly to the root zone water ~~hydraulic~~ potential (HILLFLOW with Feddes' RWU model). Simulations were compared with gas flux measurements and crop growth data from a wheat crop grown under three water supply regimes (sheltered, rain-fed and irrigated) and two soil types (stony and silty) in Western Germany in 2016. The two models showed a relatively similar performance in simulation of dry matter, LAI, root growth, RWU, gross assimilation rate, and soil water content. The Feddes model predicts more stress and less growth in the silty soil than in the stony soil, which is opposite to the observed growth. The Couvreur model better represents the difference in growth between the two soils and the different treatments. The newly coupled model (~~HILLFLOW-Couvreur's RWU-SLIMROOT-LINTULCC2-LINTULCC2-SLIMROOT-Couvreur-HILLFLOW~~) was also able to simulate the dynamics and magnitude of whole plant hydraulic conductance over the growing season. This demonstrates the importance of two-way feedbacks between growth and root water uptake for predicting the crop response to different soil water conditions in different soils. Our results suggest that a better representation of the effects of soil characteristics on root growth is needed for reliable

estimations of root hydraulic conductance and gas fluxes, particularly in heterogeneous fields. The newly coupled soil-plant model marks a promising approach but requires further testing for other scenarios regarding crop, soil, and climate.

1 Introduction

575 Soil water status is amongst the key factors that influence photosynthesis, evapotranspiration and growth processes (Hsiao, 1973). Accurate estimation of crop water stress responses is important for predictions of crop growth, yield, and water use by crop models and land surface models (Egea et al., 2011).

Crop models and land surface models lump the effects of soil water deficit on stomatal regulation and crop growth in so-called 'stress factors' (Verhoef and Egea, 2014; Mahfouf et al., 1996). Crop water stress is strongly influenced by soil water availability which in turn depends on the distribution of water and of roots in the root zone and the transpiration rate or total root water uptake. Adequate representations in simulation models of root water uptake (hereby RWU) and root distributions (Gayler et al., 2013; Wöhling et al., 2013; Zeng et al., 1998; Desborough, 1997) are therefore needed. Most macroscopic RWU models estimate the water uptake as a function of potential transpiration (i.e. the transpiration of the crop when water is not limiting) and average moisture content or soil water potential-pressure head and rooting densities (Feddes et al., 2001; van

585 Dam, 2000). However, in this representation of RWU, crucial relations between RWU model parameters and root and plant hydraulic conductances, which translate soil water potentials-pressure head to water hydraulic potentials-heads in the shoot to which stomata respond, were-are lost. Note that hydraulic heads refer to total water potentials expressed in length units, and pressure heads to the hydraulic head minus the gravitational potential or elevation. For instance, the water stress factor calculated by the Feddes model (Feddes et al., 1978) based on the soil water potentials-pressure heads involves indirect linkages between the root zone water potential-pressure head and the hydraulic head water-potential in the shoot in the sense that the water stress factors are adapted when potential transpiration rate changes. Such models like the Feddes approach represent in an indirect manner indirectly the role of the root and plant hydraulic conductance and thus require calibration for different crop types and growing seasons (Cai et al., 2018; Vandoorne et al., 2012; Wesseling et al., 1991). The conductance of the root system is an important feature of the root system and different approaches to include it in models-of-root-water-uptake RWU models were published (Quijano and Kumar, 2015; Vadez, 2014, Kramer and Boyer, 1995; Peterson and Steudle, 1993). Plant hydraulic conductance determines leaf water potentials which have a significant impact on stomatal conductance, leaf gas exchange, and leaf growth (Tardieu et al., 2014; Trillo and Fernández, 2005; Sperry, 2000; Zhao et al., 2005; Gallardo et al., 1996). Recently, some one-dimensional macroscopic RWU models based on hydraulic principles have been developed to represent water potential gradients from soil to root (de Jong van Lier et al., 2008) and within the root system (Couvreur et al., 2014). The latter approach simplified a physically based description of water flow in the coupled soil-root system accounting for the root system hydraulic properties and architecture to simple linear equations between soil water potentials-pressure heads, leaf water hydraulic potential-head, root water uptake profiles and transpiration rate that can be solved directly. It thereby avoids computation of time consuming numerical solutions of ordinary differential equations for the water flow and balance in the

595 600

Formatted: English (United States)

Formatted: English (United States)

Field Code Changed

Formatted: English (United States)

Field Code Changed

Formatted: English (United States)

Field Code Changed

605 root system that are coupled with the non-linear soil water balance partial differential equation. It uses a stomatal regulation model assuming that stomatal conductance is not influenced by the leaf water ~~potential-hydraulic head~~ as long as the leaf ~~water potential-hydraulic head~~ is above a critical ~~leaf hydraulic potential~~ threshold. Leaf water ~~potential-hydraulic head~~ is kept constant by changing stomatal conductance when the critical leaf ~~water-potential-threshold-hydraulic threshold~~ is reached. The Couvreur model also allows presenting the different stomatal regulations [i.e. isohydric and anisohydric in Tardieu and Simonneau, (1998)] (Couvreur et al., 2014, 2012).

610 Recently, inverse modelling routines using datasets of root density, ~~shoot~~-leaf area, and soil water content and potential permitted the quantification of root-related parameters of Couvreur's model (root hydraulic conductivity). Sap flow measurements were used to validate simulated RWU by the parameterized model (Cai et al., 2018; Cai et al., 2017). These studies demonstrated the close relation between the root system conductance and root growth as part of overall plant growth and its response to water stress pointing at a two-way coupling between root-water uptake and plant growth. This implies that the parameterization of root water uptake needs to be coupled to plant growth, which in turn is influenced by water stress and other factors. Plant hydraulic conductance was introduced in crop models for several field crops such as soybean (Olioso et al., 1996), winter wheat (Wang et al., 2007), or for model testing (Tuzet et al., 2003). However, plant hydraulic conductance in these studies was kept constant without reference to dynamic root growth. To our knowledge, the effect of a two-way coupling between a RWU model accounting for whole plant hydraulic regulation and a crop growth model has not been studied yet. It is unclear whether such a coupled model improves the simulation of crop growth and development, CO₂ and H₂O fluxes. In this study, we coupled the Couvreur's RWU model (Couvreur et al., 2014; Couvreur et al., 2012) with the existing crop growth model LINTULCC2 (Rodriguez et al., 2001) to consider the whole plant hydraulic conductance from root to shoot. The dynamics of root and shoot growth under varying soil water availability are explicitly represented by the coupled model. The overall aim of the study was to investigate whether consideration of plant hydraulic conductance can improve the simulation of CO₂ and H₂O fluxes, and crop growth in biomass, roots, and leaf area index of the same crop that is grown in two different soils and for three different water application regimes. To achieve this aim, three objectives were addressed: (i) analyse and compare the predictive quality of a crop growth model coupled with a RWU model that considers plant hydraulics (Couvreur RWU model) and a model that does not consider plant hydraulics (Feddes RWU model), (ii) compare the simulated plant hydraulic conductances for the different growing conditions with direct estimates of these conductances from measurements, and (iii) analyse the sensitivity of RWU and crop growth to the Couvreur RWU and root growth model parameters (root hydraulic conductance, critical leaf ~~water-potential-hydraulic~~ threshold, and specific weight of seminal and lateral root).

2 Materials and Methods

2.1 Location and experimental set-up

635 The study area was located in Selhausen in North Rhine-Westphalia, Germany (50°52'N, 6°27'E). The study field is slightly inclined with a slope of around 4° and characterized by a strong gradient in stone content along the slope (Stadler et al., 2015).

Two rhizotrones were set up in the field: the upper site with stony soil (hereby F1) contains up to 60% gravel by weight while in the lower site with silty soil (hereby F2) the gravel content was approximately 4%. At each study site the effects of three different water treatments on growth and fluxes were investigated (sheltered – P1, rainfed – P2, and irrigated – P3) (Fig. 1).

640 Each treatment was 3.25 m wide and 7 m long. The treatments bordered each other along 7-m-long side. Further information on the field experiment and set-up are presented in Cai et al., (2016), Stadler et al., (2015), and Cai et al., (2018). Irrigation was applied two times: on 22 May and 26 May 2016 in the irrigated plots (FIP3 and F2P3) during the growing season using dripper lines. The dripper lines (Model T-Tape 510-20-500, Wurzelwasser GbR, Münzenberg, Germany) were installed with 0.3-m intervals and parallel to crop rows. The non-transparent plastic shelter was manually covered (11 times) during rainfall and removed when rain stopped to induce water stress. On the sheltered days, radiation was assumed to be zero for the sheltered plots. Winter wheat (*Triticum aestivum* cv. Ambello) was sown with a density of 350-370 seed m⁻² on 26 October 2015 and harvested on 26 July 2016 in both the stony (F1) and silty (F2) parts of the field. Fertilizers were applied at a rate of 80 kg N + 60 kg K₂O + 30 kg P₂O₅ per hectare on 15 March 2016. Nitrogen was further added on 2 May and 7 June 2016 with 60 and 50 kg N per hectare, respectively. Weeds and pests were controlled according to standard agronomic practice.

650 [Insert Fig. 1 here]

2.2 Measurements

2.2.1 Soil water measurement, soil property, and root growth

Soil water content and soil water potential were measured hourly by home-made time domain reflectometer (TDR) probes (Cai et al., 2016), tensiometers (T4e, UMS GmbH), and dielectric water potential sensors (MPS-2 matric potential and temperature sensor, Decagon Devices), respectively. Sensors were installed at 10, 20, 40, 60, 80 and 120 cm depth. Root measurements were taken with a digital camera (Bartz Technology Corporation) repeatedly from both left and right sides at 20 locations along 7 m-long horizontally installed minirhizotubes (clear acrylic glass tubes with outer and inner diameters of 64 and 56 mm, respectively). The calibration of the sensors, root growth observation, and post processing of the data ~~was~~ were described in detail in Cai et al., (2016) and Cai et al., (2017).

660 2.2.2 Sap flow, leaf water potential-hydraulic head, and gas fluxes measurement

Five, three, and five sap flow sensors (SAG3) (Dynamax Inc., Houston, USA) were installed in the irrigated, rain-fed and sheltered treatments, respectively, at the beginning of wheat anthesis when stem diameters ranged between 3-5 mm. Vertical and horizontal temperature gradients, (dT) of each sensor were recorded at 10 minute intervals with a CR1000 data logger and two AM 16/32 multiplexers (Campbell Scientific, Logan, Utah). Sensor heat inputs were controlled by voltage regulators controlled by the CR1000 data logger. The raw signal data was aggregated to 30 minutes intervals and sap flow ~~was~~ calculated following Langensiepen et al., (2014). The number of tillers per square meter was counted every two weeks during the operation period of sap flow sensors (26 May – 23 July 2016). Tiller numbers were used to upscale the sap flow of single tiller (g h⁻¹) to canopy transpiration rate (mm h⁻¹ or mm d⁻¹).

Leaf stomatal conductance and leaf water potential-hydraulic head was measured every two weeks from 7 am-AM to 8 pm PM under clear and sunny conditions from tillering (20 April) to the beginning of maturation (29 June 2016). Stomatal conductance to water vapor of three to four upmost fully developed leaves were measured using a LICOR 6400 XT device (Licor Biosciences, Lincoln, Nebraska, USA) with a reference CO₂ concentration of 400 ppm, flow rate of 500 (μmol s⁻¹), and using real-time records of photosynthetic active radiation, vapor pressure deficit, and leaf temperature provided by the instrument. Then Three to four upmost fully developed leaves from three to four different plants the leaves -were quickly detached by a sharp knife to measure leaf water potential-pressure head with a digital pressure chamber (SKPM 140/ (40-50-80), Skye Instrument Ltd, UK).

Plant hydraulic conductance in crop species can be estimated by measuring the transpiration and the root zone and leaf water potentials-hydraulic heads (Tsuda and Tyree, 2000). In our study, we calculated the conductance according to Ohm's law by dividing the hourly sap flow by the difference between effective root-zone water-potentialhydraulic head and leaf water potentialhydraulic head. The effective root zone water-potentialhydraulic head was calculated based on hourly measured soil water hydraulic head potential and measured root length density (cm cm⁻²) at 6-six depths (10, 20, 40, 60, 80, and 120 cm) in the soil profile following Eqs. (8) and (10) (see Section 2.3.4). During one measurement day, 6 hourly values of the conductance were obtained from measurements between 11 AM to 4 PM. The average and standard deviation of these hourly measurements were calculated for each measurement day. Yet, the hydraulic conductance can vary within short time periods due to the role of aquaporins (Maurel et al., 2008; Javot and Maurel, 2002; Henzler et al., 1999) or ABA regulation (Parent et al., 2009), and xylem cavitation (Sperry et al., 1998). We assumed however a constant plant hydraulic conductance during the day.

Canopy gas exchange was measured hourly on the same days when leaf water potentials-pressure heads were measured with a closed chamber system (Langensiepen et al., 2012). CO₂ concentration was derived with a regression approach by Langensiepen et al., (2012). Because we were interested in comparing measured with calculated hourly instantaneous gross assimilation by the newly coupled root: shoot model (LINTULCC2 with other subroutines), the total soil respiration (i.e. heterotrophic organisms and root respiration) was subtracted from the instantaneous canopy CO₂ exchange rate measured by the closed chamber. The total soil respiration was calculated based on measured soil temperature, soil water content at 10 cm soil depth, and leaf area index from crop using the fitted parameters derived from the same field and soil types (Prolingheuer et al., 2010). The calculated total soil respiration was compared and validated with the measured values in the same field in the previous years from Stadler et al., (2015).

2.2.3 Crop growth

Crop growth information was collected bi-weekly from 20 April until harvest 26 July 2016. Leaf area index and crop biomass were measured by harvests of two rows (1 m each) for each treatment. Leaves were separated into green leaves and brown leaves, and the brown and green leaf area was measured using a leaf area meter (LI-3100C, Licor Biosciences, and Lincoln, Nebraska, USA). The above-ground biomass was measured using the oven drying method. Samples were first weighed in total,

then separated into different plant organs (green leaf, brown leaf, stem, ear, and grain) and weighed. Subsamples were afterward extracted from these samples, weighed, dried in an oven at 105 °C for 48 hours and weighed again for determining dry matter. At the end of growing season, four replicates of one square meter of plants were harvested from the plots to determine grain yield and harvest index.

2.3 Model description

2.3.1 Description of the original ~~Lintulcc~~ LINTULCC crop model

We used the crop model LINTULCC2 (Rodriguez et al., 2001). LINTULCC2 couples photosynthesis to stomatal conductance and can perform a detailed calculation of leaf energy balances (Rodriguez et al., 2001) (see Appendix A). This model was validated and compared with different crop models for spring wheat and used to simulate the effects of elevated CO₂ and drought conditions (Ewert et al., 2002; Rodriguez et al., 2001). LINTULCC2 calculates phenology, leaf growth, assimilate partitioning, and root growth following the procedure outline in Rodriguez et al., (2001).

In LINTULCC2, the assimilation rate of the sunlit and shaded leaf is calculated using the biochemical model of Farquhar and Caemmerer (1982). Stomatal conductance (g_s) was calculated according to the model of Leuning (Leuning, 1995) for sunlit and shaded leaves separately. In LINTULCC2 CO₂ uptake is calculated as a function of CO₂ demand by photosynthesis, and the ambient concentration of CO₂, using the iterative methodology proposed by Leuning (1995) (Appendix A). For the sake of simplification, in LINTULCC2, the internal leaf CO₂ concentration, C_i , is initially assumed as 0.7 times the atmospheric CO₂ concentration C_a (Vico and Porporato, 2008; Rodriguez et al., (2001); Jones, 1992). Then, the light saturated photosynthetic rate of sunlit and shaded leaves (AMAXsun, and AMAXshade, $\mu\text{M CO}_2 \text{ m}^{-2} \text{ s}^{-1}$), and the quantum yield for sunlit and shaded leaves (EFFsun, and EFFshade, $\mu\text{M CO}_2 \text{ MJ}^{-1}$), are calculated iteratively (Farquhar et al., 1980; Farquhar, 1982). This iterative loop ends when the difference in calculated internal CO₂ mole fraction between two consecutive loops is $< 0.1 \mu\text{mol mol}^{-1}$ (Appendix A). Based on a fraction of sunlit (and shaded) leaf area and LAI leaf area index (LAI), the leaf stomatal resistance of sunlit and shaded leaves was integrated over the canopy leaf area to the canopy resistance (r_s) (Appendix B).

The canopy resistance, crop height, and calculated crop albedo (depending on both crop and soil water content of the surface layer) and the surface energy balance were used to calculate potential crop evapotranspiration (ETP – mm h^{-1}) using the Penman-Monteith equation (Allen et al., 1998) (see Appendix B). The obtained potential surface evapotranspiration is then split into evaporation and potential transpiration using:

$$T_{pot} = ETP(1 - e^{-kLAI}) \quad (1)$$

where k is the light extinction coefficient [0.6 in this study (Faria et al., 1994; Mo and Liu, 2001; Rodriguez et al., 2001)].

Field Code Changed

730 T_{pot} (mm h⁻¹) represents by definition the transpiration of the crop that is not limited by the root zone water ~~potential~~hydraulic head. In section 2.3.4 it is explained how the actual transpiration, T_{plant} (mm h⁻¹), is calculated as a function of the potential transpiration and the root zone soil water ~~potential~~pressure head. The ratio T_{plant}/T_{pot} defines the water stress factor f_{wat} , which is used in the photosynthesis model:

$$f_{wat} = \frac{T_{plant}}{T_{pot}} \quad (2)$$

Originally, LINTULCC2 runs at daily time steps (which allows for the within day variations in temperature, radiation and vapor pressure deficit). LINTULCC2 requires daily maximum and minimum temperature, actual vapor pressure, rainfall, wind speed, and global radiation. In order to capture the diurnal response of stomata, we modified the time step of the photosynthesis and stomatal conductance subroutine from daily to hourly, while daily time steps were kept in the remaining subroutines (phenology, leaf growth, ~~and~~ biomass partition).

2.3.2 Root growth model

740 Root growth was simulated using SLIMROOT (Addiscott and Whitmore, 1991). The vertical extension of the seminal roots and the distribution of the lateral roots within the soil profile depend on the root biomass, the soil bulk density, the soil water content calculated by Hillflow1D (Bronstert and Plate, 1997), and the soil temperature computed by STMPsim (Williams and Izaurrealde, 2005). The supply of assimilates from the shoot (RWTR) (g m⁻² d⁻¹) is given by a partitioning table based on the thermal time (van Laar et al., 1997) that is used to calculate the vertical penetration of seminal and lateral roots. The assimilate allocation for seminal root growth (ASROOT) is constrained by daily supply of assimilates from the shoot RWRT (g m⁻² d⁻¹) and the demand of assimilates from seminal roots (ASROOT_{demand}).

$$ASROOT = \min(ASROOT_{demand}, RWRT) \quad (3)$$

ASROOT_{demand} is a function of the number of seminal roots per square meter (NSROOT) which depends on the number of emerged plants per square meter and the number of seminal roots per plant; the specific weight of seminal root WSROOT (g m⁻¹); and the daily elongation rate of seminal roots RSROOT (m d⁻¹):

$$ASROOT_{demand} = RSROOT * WSROOT * NSROOT \quad (4)$$

750 RSROOT depends on the soil temperature and is constrained by a maximal elongation rate, RSROOT_{max} and the soil temperature depend rate which is an empirical function of the soil temperature of the deepest layer where roots are growing, TBOTLAYER (K) (Jamieson and Ewert, 1999):

$$RSROOT = \min(RSROOT_{max}, TBOTLAYER * RTFAC) \quad (5)$$

where RTFAC is the temperature factor driving the penetration of seminal roots (m K⁻¹ d⁻¹) and TBOTLAYER (K) the soil temperature of the deepest layer where roots are growing. When soil temperature is below or equal to 0°C, no seminal growth

Formatted: Font: Not Italic

755 occurs. The maximum daily elongation rate of seminal roots, $RSROOT_{max}$ was set at 0.03 m d^{-1} for wheat according to Watt et al., (2006).

The daily increment in seminal root length (SRLIR - $\text{m m}^{-2} \text{ d}^{-1}$) is defined as:

$$SRLIR = ASROOT/WSROOT \quad (6)$$

760 Lateral roots are simulated when the root biomass supplied by the shoot is greater than the assimilate demand of seminal roots ($RWRT > ASROOT_{demand}$). Lateral root biomass is distributed stepwise from the top layer to the deepest soil layer with seminal roots.

Roots start to die after anthesis. Since the specific weight of the roots of cereal crops varies with soil strength (Colombi et al., 2017; Lipiec et al., 2016; Hernandez-Ramirez et al., 2014; Merotto Jr and Mundstock, 1999), we chose different specific weights for the stony (F1) and silty soil (F2) from the range that was observed by Noordwijk and Brouwer (1991) and Jamieson and Ewert (1999) in soils with different soil strength (Appendix C).

765 2.3.3 Physically based soil water balance model

HILLFLOW 1D was chosen for calculating the water ~~potentials-pressure heads~~ in the soil and how they change with depth and time as a function of the precipitation, soil evaporation, RWU, and water percolation at the bottom of the simulated soil profile (Bronstert and Plate, 1997). HILLFLOW 1D calculates soil water content and water fluxes by numerically solving the Darcy equation for unsaturated water flow in porous media (Bronstert and Plate, 1997). The relations between soil water ~~matric potential~~ ~~hydraulic~~ head, water content and hydraulic conductivity are described by the Mualem-van Genuchten functions (van Genuchten, 1980). The parameters of these functions, i.e. the soil hydraulic parameters, for the different soil layers and the two sites were taken from (Cai et al., 2018) (Appendix D). In this study, a soil depth of 1.5 m vertically discretized into 50 layers was considered. A free drainage bottom boundary and a mixed flux-matric potential boundary at the soil surface were implemented. The mixed upper boundary condition prescribes the flux at the soil surface by the precipitation and evaporation rates as long as the ~~matric potential~~ ~~soil water pressure~~ heads are not above or below critical heads. When these heads are reached, the boundary conditions are switched to constant ~~matric potential~~ ~~pressure head~~ boundary conditions.

2.3.4 Feddes' and Couvreur's root water uptake models

780 The Feddes RWU model (Feddes et al., 1978) (See Appendix E) was already built in the HILLFLOW 1D model (Bronstert and Plate, 1997). We implemented the Couvreur RWU model (Couvreur et al., 2014a; Couvreur et al., 2012) into HILLFLOW. Both models, T_{plant} is calculated ~~for each in both~~ models from the sum of the simulated RWU in the different soil layers and used to calculate the water stress factor (f_{wat}) following Eq. (2), which was used in the photosynthesis model. In the Feddes model, root water uptake from a soil layer is proportional to the normalized root density, NRLD (m^{-1}), in that layer and is multiplied by a stress function α that depends on the ~~matric potential~~ ~~soil water pressure~~ head, ψ_m (m), in that soil layer and the potential transpiration rate (see Appendix E for the definition of α):

$$RWU_i = \alpha(\psi_{m,i}, T_{pot})T_{pot}NRLD_i\Delta z_i \quad (7)$$

785 where $NRLD_i$ is calculated from the root length density, RLD ($m\ m^{-3}$) and discretized soil depth Δz_i (m) as:

$$NRLD_i = RLD_i / \sum_{i=1}^N RLD_i \Delta z_i \quad (8)$$

The parameters of the α stress functions model were taken from (Cai et al., 2018) (See Appendix C). According to Eq. (7), the reduction of water uptake in a ~~certain given~~ layer depends on the ~~matric potential head~~ soil water pressure head in that layer only and does not influence the water uptake in other layers. This means that a reduced water uptake in dried out soil layers directly leads to a reduction of the total root water uptake and plant transpiration and is not compensated by increased uptake in other layers where there is still ~~sufficient~~ water available.

In the Couvreur model, ~~which is based on a mechanistic description of water flow in the coupled soil-plant system~~, the root water uptake in a ~~certain given~~ soil layer is related to the water potentials in the root system and root water uptake in other soil layers so that compensatory uptake is considered in this model. Root water uptake in a certain layer is obtained from:

$$RWU_i = T_{plant}NRLD_i\Delta z_i + K_{comp}(\psi_i - \psi_{sr})NRLD_i\Delta z_i \quad (9)$$

795 where ψ_i (m) is the total ~~water potential~~hydraulic head (or hydraulic head which is the sum of the ~~pressure head~~ matric and gravitation potential heads) in layer i , ψ_{sr} (m) is the average hydraulic head in the root zone and K_{comp} (d^{-1}) is the root system conductance for compensatory uptake. The first term of Eq. (9) represents the uptake from that soil layer when the hydraulic head is uniform in the root zone and the second term represents the increase or decrease of uptake from the soil layer due to a respectively higher and lower hydraulic head in layer i than the average hydraulic head. The average root zone hydraulic head is calculated as the ~~weight~~ed average of the hydraulic heads in the different soil layers as:

$$\psi_{sr} = \sum_{i=1}^N \psi_i NRLD_i \Delta z_i \quad (10)$$

800 The plant transpiration rate is the minimum of the potential transpiration rate and the transpiration rate, $T_{threshold}$ ($mm\ h^{-1}$), when the hydraulic head in the leaves reaches a threshold value, $\psi_{threshold}$ (m) that triggers stomatal closure:

$$T_{plant} = \max(0, \min(T_{pot}, T_{threshold})) \quad (11)$$

$T_{threshold}$ is calculated from ~~the~~ difference between the root zone hydraulic head and the threshold hydraulic head in the leaves $\psi_{threshold}$ that is multiplied by the plant hydraulic conductance, K_{plant} as:

$$T_{threshold} = K_{plant}(\psi_{sr} - \psi_{threshold}) \quad (12)$$

In our study, we used the a critical leaf hydraulic head, $\psi_{threshold}$ of -200 m (equivalent to -2 MPa) (Cochard, 2002; Tardieu and Simonneau, 1998). The original Couvreur model only considers the hydraulic conductance from the roots to the plant collar, K_{rs} , by assuming that the hydraulic resistance from plant collar to leaves is minor as compared to root system resistance. The shoot hydraulic resistance could be large in some crop plants (Gallardo et al., 1996) or in trees (Domec and Prunyn, 2008; Tsuda and Tyree, 1997). In order to simulate the leaf water **potentialhydraulic head**, the whole plant hydraulic conductance (K_{plant}) needs to be used. The whole plant hydraulic conductance could be estimated from different components (i.e. soil to root, stem to leaf) following an approach from Saliendra et al., (1995) or a more complex attempt by Janott et al., (2011). Because hydraulic data from plant collar to leaf are rare and difficult to obtain and account for differing species characteristics and environmental conditions, for the sake of simplification, we derived K_{plant} (d^{-1}) from the root hydraulic conductance ($K_{rs,doy}$) assuming that K_{plant} is a constant fraction β of $K_{rs,doy}$ (d^{-1}):

$$K_{plant} = \beta K_{rs,doy} \quad (13)$$

We used the measured plant hydraulic conductance from sap flow, leaf water **potentialhydraulic head**, soil water **potentialpressure head**, and root observation (Section 2.2.1 above) in the lower rainfed plot to calibrate β which was then applied for all plots (Appendix C). K_{plant} and K_{rs} in anisohydric wheat are influenced by soil water availability and crop development. We followed the approach of Cai et al., (2017) to estimate the root hydraulic conductance ($K_{rs,doy}$) and compensatory root water uptake (K_{comp}) based on the total length of the root system below a unit surface area, $TRLD_{doy}$ ($m\ m^{-2}$), at a given day of year (DOY) (Eq. 14), which is the output from SLIMROOT:

$$TRLD_{doy} = \sum_i^N RLD_{i,doy} \Delta z_i \quad (14)$$

Assuming the same conductance for all root segments, the root system conductance scales with the TRLD:

$$K_{rs,doy} = K_{rs,normalized} TRLD_{doy} \quad (15)$$

where $K_{rs,normalized}$ ($d^{-1}\ cm^{-1}\ cm^2$) is the root system conductance per unit root length per surface area. For $K_{rs,normalized}$, we took the average value that was obtained by Cai et al., (2018) for the stony soil (F1) and silty soil (F2) sites: $0.2544 \cdot 10^{-5}$ ($d^{-1}\ cm^{-1}\ cm^2$) (Appendix C).

Many studies included hydraulic conductance along the soil-plant-atmosphere pathway to simulate water transport (Verhoef and Egea, 2014; Wang et al., 2007; Tuzet et al., 2003; Olioso et al., 1996). However, root and plant hydraulic conductance in

Formatted: German (Germany)

these studies were assumed constant. In our work, the plant hydraulic conductance varied following the shoot and root development in the growing season.

2.3.5 Coupling of water balance and root water uptake models with the crop model

We carried out a comprehensive comparison of the following modelling approaches for simulating CO₂ and H₂O fluxes and crop growth (Fig. 2):

- HILLFLOW 1D - Couvreur's RWU - SLIMROOT - ~~LintulCC2-LINTULCC2~~ (Co) ;
- HILLFLOW 1D - Feddes' RWU - SLIMROOT - ~~LintulCC2-LINTULCC2~~ (Fe)

The photosynthesis and stomatal conductance subroutines, RWU and HILLFLOW 1D water balance model, and evaporative demand (ETP) were run or specified with hourly time steps, while phenology, leaf growth, root growth, and biomass partitioning were updated daily. For a certain hourly time step $\Delta t_i = t_i - t_{i-1}$, different modules were solved in the following sequence. First, LINTULCC2 was used with a water stress factor $fwat = 1$ to calculate the leaf and canopy resistance, and the potential transpiration rate. T_{pot} was then used in HILLFLOW 1D to calculate the soil water pressure head changes, water content changes, the actual transpiration, and $fwat$ during the time step. LINTULCC2 was then run again using the $fwat$. The leaf conductance and assimilation rate were calculated. For the next time step, the same loop was run and hourly assimilation was accumulated to a daily value. Daily assimilation rates were used in modules that run with a daily time step. For instance, modules of LINTLCC2 that calculate assimilate partitioning which is used to calculate shoot (LAI) development and passed to SLIMROOT to simulate root development (Fig. 2). Before comparing these modelling approaches, we calibrated the original LINTULCC model using the data from the rainfed plots in the silty soil (F2P2). The model is firstly calibrated to make sure the model properly described the phenology. Two parameters (minimum thermal sum from sowing to anthesis and thermal sum from anthesis to maturity (°C d)) were used for phenology calibration based on information of sowing, anthesis, and maturity dates. The model was then calibrated using time series of LAI, biomass, and gross assimilation rate through the change of maximum carboxylation rate at 25 °C (VCMAX25), critical leaf area index (LAICR), and relative growth rate of leaf area during exponential growth (RGRL) parameters. Before comparing these modelling approaches, we calibrated the original LINTULCC2 model to make sure the model properly described the phenology, LAI, and biomass using the data from the rainfed plot in the silty soil (F2P2). The same crop parameters and soil parameters were applied for both model configurations (Appendix C, D). All presented flux data (soil water flux, gross assimilation rate, sap flow, stomatal conductance, and leaf water potential pressure head) and the simulated outputs were converted from local time to coordinated universal time (UTC) to avoid the confusion in interpretation.

[Insert Fig. 2 here]

2.4 Criteria for model comparison and evaluation

We analysed the performance of two modelling approaches following the approach from (Willmott, 1981): (i) correlation coefficient (r) (Eq. 16); (ii) the degree to which simulated values approached the observations or index of agreement (I) defined in Eq. (17). This value varies from 1 (for perfect agreement) to 0 (for no agreement); (iii) the root mean square errors (RMSE)

860 was computed to **measure the differences characterize the difference** between simulated value and observed data (Eq. 18);

$$r = \frac{\sum_{i=1}^n (Sim_i - \overline{Sim})(Obs_i - \overline{Obs})}{\sqrt{\left[\sum_{i=1}^n (Sim_i - \overline{Sim})^2\right] \left[\sum_{i=1}^n (Obs_i - \overline{Obs})^2\right]}} \quad (16)$$

$$I = 1 - \left[\frac{\sum_{i=1}^n (Sim_i - Obs_i)^2}{\sum_{i=1}^n (|Sim_i - \overline{Obs}| + |Obs_i - \overline{Obs}|)^2} \right] \quad (17)$$

$$RMSE = \sqrt{\frac{\sum_{i=1}^n (Sim_i - Obs_i)^2}{n}} \quad (18)$$

where Sim and Obs are simulated and measured variables; i is the index of a given variable; \overline{Obs} and \overline{Sim} is the mean of the simulated and measured data; and n is the number of observations;

2.5 Sensitivity analysis

The parameters of the SLIMROOT root growth model and the Couvreur RWU model were derived from literature data.

865 However, these parameters **may beare** uncertain and vary between different wheat varieties. In order to evaluate the effect of these parameters on the simulated crop growth and root water uptake, we carried out a sensitivity analysis.

In a first set of simulations, the root length normalized root system conductivity $K_{rs, \text{normalized}}$ was varied from 0.1 to 40 times the $K_{rs, \text{normalized}} = 0.2554 \cdot 10^{-5} \text{ cm d}^{-1} \cdot (\text{d}^{-1} \cdot \text{cm}^{-3})$ that was estimated by Cai et al., (2018). The root system hydraulic conductance is related to the total root length, which depends on the specific weight of lateral and seminal roots. These two

870 parameters are rarely reported, especially for field grown wheat (Noordwijk and Brouwer, 1991). The range of observed specific weight of lateral root in wheat was reported in the range of 0.00406 to 0.00613 g m^{-1} (Noordwijk and Brouwer, 1991).

Huang et al., (1991) found that the specific weight of seminal root of winter wheat grown under controlled soil chamber conditions decreased from 0.023 to 0.0052 g m^{-1} when air temperature increased from 10 to 30°C. The values of 0.015 and 0.0035 g m^{-1} are often used for specific weights of seminal and lateral roots, respectively in crop growth simulations of wheat

875 cultivars (Mboh et al., 2019; Jamieson and Ewert, 1999). In a second set of simulations, the specific weight of lateral roots was subjected to change from 0.002, 0.003, 0.0035, 0.004, 0.005, 0.006, and 0.007 g m^{-1} while specific weight of seminal roots was the same (0.015 g m^{-1}) for all simulations. For the third set of simulations, specific weight of lateral root was kept at 0.0035

g m⁻¹ while the specific weights of seminal root varied from 0.005, 0.0075, 0.01, 0.0125, 0.015, 0.0175, 0.02, and 0.0225 g m⁻¹. In the last sensitivity exercise, the critical leaf ~~water potential-hydraulic head threshold~~ ($\Psi_{\text{threshold}}$) ~~was~~ ~~were~~ ~~was~~ varied between -120 m and -260 m.

3 Results and discussion

In the first section, we discuss the performance of the two coupled root-shoot models with Couvreur RWU model (Co model) and Feddes RWU model (Fe model). The comparative analysis firstly focuses on simulating crop growth and root development under different water conditions and soil types. Next, the simulated transpiration reduction, soil water dynamics, RWU, and gross assimilation rate are presented and discussed. The ~~explicitly simulated~~ K_{plant} ~~is explicitly simulated~~ by the Co model in the different soils and treatments [and](#) is compared with direct estimates of K_{plant} from measurements. In the second part, we discuss the sensitivity analysis of the Co model to understand the effects of changing $K_{\text{rs, normalized}}$, specific weight of seminal and lateral root, and $\Psi_{\text{threshold}}$ on the simulated biomass growth and RWU ~~under-in~~ different soils and [under different](#) water regimes.

3.1 Comparison of Couvreur and Feddes's RWU model

3.1.1 Root and shoot (biomass and LAI) growth

Fig. [2-3](#) shows the dry matter and LAI simulated by the Co and Fe model versus the measured data. The difference between the two samples of the two different rows for each sampling day indicated the heterogeneity in crop growth even within a small treatment plot. Biomass and LAI simulated by the Co and Fe models were in [close-fair](#) agreement with observations. The r^2 of Co and Fe models were 0.91 and 0.86, respectively, for biomass while 0.76 and 0.75, respectively, for LAI (Table 1). However, both models overestimated dry matter and LAI production in the irrigated and rainfed stony plots whereas biomass and LAI were underestimated in the sheltered silty plot. This suggests that water stress in the sheltered silty plot was overestimated. For the irrigated stony soil plot, in which the water content stayed high due to the frequent rainfall events and the additional irrigation, it is unlikely that the lower growth is due to water stress. The later start of the growth after the winter could be due to the effects of soil strength and lower soil temperature on crop development in the stony field that were not captured by the model. Soil hardness could constrain root growth while the higher stone content possibly resulted in slower warming up of the soil in spring than the silty soil which in turn slowed down root and crop development.

[Insert Fig. [2-3](#) here]

For the stony plots, the Fe and Co models gave similar results whereas for the silty soil, the Co model reproduced the biomass and LAI better than the Fe model. Although the statistical parameters (r^2 and RMSE) for the silty soil plots show only a slightly better fit of the Co than of the Fe model, there is a remarkable qualitative difference between the models. The Fe model simulated lower biomass and leaf area in the silty soil than in the stony soil, which is opposite to the observations. The Co model simulated similar biomass and LAI in the irrigated and rainfed plots of the silty and stony soils and higher biomass and LAI in the sheltered plot in silty soil than in the stony soil, which is in closer agreement with the observed differences in

910 biomass and LAI between the two soils. The simulated effect of the soil type on the crop growth was qualitatively correct for the Co model but incorrect for the Fe model.

[Insert Table 1 here]

Fig. 3-4 displays the observed root length densities from minirhizotube observations and the simulated ones. Higher root length densities were observed and simulated in the silty soil than in the stony soil. The model simulated smaller root densities in the stony soil because a larger specific weight of the roots was considered for the stony than for the silty soil. The simulated root density profiles showed the highest root densities near the surface whereas the observed profiles, especially in the silty soil, showed higher densities in the deeper soil layers. The model simulated smaller root length densities in the sheltered than in the other plots of both the stony and silty soils. This is a consequence of the lower biomass growth that was simulated in the sheltered plots. For the stony soil, this corresponds with the observations that also showed lower root length densities in the sheltered than in the other plots. However, for the silty plot, the opposite was observed. For both the simulations and the observations, we compared the ratio of total root lengths in a certain plot and treatment to the total root length in rainfed stony plot FIP2 (Appendix F). In the stony plots the ratios of the observed total root length to the reference were close to 1 but the simulated total root length in the sheltered plot was smaller than one. The ratios of the total root lengths in the silty plot to the reference were for all plots larger than one. Nevertheless, the ratios of observed root lengths were larger (2.27 - 4.03) than those of the simulated ones (1.04 - 1.67). The observed ratios were larger for the sheltered plot than for the other plots in the silty soil whereas the opposite was simulated by the models. -Predefined ratios of root and shoot biomass allocation for a given growth period and a source driven root growth (van Laar et al., 1997) (Goudriaan and van Laar, 1994) in our models do not allow a shift in carbon allocation to root (for more root growth) in response to water stress. However, this should be not be too emphasized too much because the observed imaged root data from minirhizotubes for driving the root length might have potential errors and uncertainties (Cai et al., 2018).

[Insert Fig. 3-4 here]

3.1.2 Transpiration reduction, soil water dynamic, RWU, and gross assimilation rate

Fig. 4a-5a and 4b-5b show the simulated reduction of the transpiration compared to the potential transpiration, $f_{\text{war}}f_{\text{wat}}$, simulated by the Fe and Co models (mid of March until harvest) and Fig. 4e-5c and 4d-5d show the simulated potential and the simulated and measured actual transpiration rates from the end of April until harvest. The Fe model simulated more water stress than the Co model and a more pronounced and earlier stress in the silty than in the stony soil. As a consequence, the simulated transpiration rates by the Fe model were generally lower than the simulated ones by the Co model. According to the $f_{\text{war}}f_{\text{wat}}$ factors, also the Couvreur model simulated more water stress in the silty soil than in the stony soil. The effect of $f_{\text{war}}f_{\text{wat}}$ on the cumulative transpiration and growth depends also on the timing of the lower $f_{\text{war}}f_{\text{wat}}$ values. At the beginning of the growing season when the LAI and potential transpiration are low, the impact of a lower $f_{\text{war}}f_{\text{wat}}$ on the cumulative transpiration and growth is lower than later in the growing season. These results are in contrast with findings by Cai et al., (2017) and Cai et al., (2018) who found that there was no water stress simulated in the silty soil in 2014 by the Co and Fe

models. However, the studies from Cai et al., (2018) used the measured root distributions instead of the simulated ones from the root-shoot model. Therefore, in their simulations, the crop had more access to water in the deeper soil layers. Second, they used the Feddes-Jarvis model, which accounts for root water uptake compensation. This could explain why they did not simulate water stress in the silty plot with the Feddes model. Thirdly, weather conditions and irrigation applications were different in their study in 2014 (less ~~drier~~^{drier}) from our experimental season in 2016.

[Insert Fig. 4-5 here]

According to Fig. 4e-5c and 4d5d, during the time when sap flow could be measured (from end of May until harvest), the stress factors did not differ a lot between the Fe and Co models. For the rainfed and irrigated plots in the silty soil, the Fe model predicted a stronger reduction in transpiration near the end of the growing season than the Co model. This resulted in a smaller cumulative transpiration predicted by the Fe than by the Co model over the measurement period in these treatments (Fig. 56). Although this gives the impression that the Co model is better in agreement with the measurements in these treatments, Fig. 4d-5d indicates that this is due to compensating errors. Both models underestimate the measured sap flow in the beginning of the measurement period and overestimate it towards the end, and the Co model overestimates more than the Fe model. This overestimation is due to an overestimation of the LAI by both models near the end of the growing season (Fig. 2b3b). The reduction of the transpiration in the sheltered plots of the two soils compared to the other treatments is predicted relatively well but the Fe model predicted more stress and a stronger reduction in transpiration than the Co model, especially in the silty soil. For this treatment, the Co model, which simulated less stress (larger $f_{\text{war}}-f_{\text{wat}}$ factors), predicted the cumulative transpiration and how it differed between the two soil types better than the Fe model.

[Insert Fig. 5-6 here]

Simulated transpiration in all treatments and both soils are plotted versus the sap flow measurements in Fig. 67. On average, the two models slightly underestimated measured T_{act} (Fig. 4e-5c and 4d5d). This was also found in the study by Cai et al., (2018) where sap flow was measured in winter wheat in 2014. However, in their study, there was a rather constant offset between the simulations and the sap flow data. One reason could be that in our study we used the simulated LAI values whereas Cai et al., (2018) used the measured LAI values. In the stony plots, the measured LAIs are overestimated by the simulations so that one would expect an overestimation of the transpiration by the model. The opposite holds true for the silty plot. The overestimation of the LAI at the end of growing season resulted in an overestimation of the transpiration in non-sheltered plots in both soil types. Because of the small size and hollow stem of wheat plants (Langensiepen et al., 2014), it is difficult to install the micro-sensors and measure the temperature variation for the thin wheat stem with high time frequency under ambient field conditions. In addition, the sap flow in a single tiller is also influenced by spatial variation in environmental conditions. The variability of stem development also results in a significant stem-to-stem variability in sap flow (Cai et al., 2018). The r^2 of simulated RWU from the Co and Fe models versus sap flow are 0.62 and 0.66, respectively (Table 1 and Fig. 6a7a) indicating that our coupled models have ~~adequate~~^{adequate}-~~fair~~^{fair} performance in RWU simulation. Measuring gas exchange with closed chamber concentration measurements can significantly alter the microclimatic conditions within the chamber, especially at times of

high exchange rate. However using regression functions at the starting point of measurement intervals reduces absolute errors (Langensiepen et al., 2012). The simulated gross assimilation rate (Pg) from two models matched relatively well with the gross assimilation rate measured by a manually closed-canopy chamber with r^2 of 0.63 and 0.61 for Co and Fe, respectively (Table 1 and Fig. 6b7b).

980 [Insert Fig. 6-7 here]

The method that we used for modelling the canopy resistance used in the Penman-Monteith has been reported for both short and tall crops (Dickinson et al., 1991; Kelliher et al., 1995; Irmak & Mutiibwa, 2010; Perez et al., 2006; Katerji et al., 2011; Srivastava et al., 2018). The fair agreement of RWU to sap flow in our study indicates the proper estimate of ETP based on the crop canopy resistance (with $f_{wat} = 1$) in winter wheat. The direct calculation of crop canopy resistance in our work allows to capture physiological characteristics responses of the crop (stomatal conductance) which depends onto solar radiation, temperature, and vapor pressure deficit (Eqn. A5). In addition, this approach also avoids use of calculating grass reference evapotranspiration based on a constant canopy resistance.

The differences in simulated stress between the different models were more pronounced in May (Fig. 45) when no sap flow data were available. The Co model predicted less stress and more RWU than the Fe model in May, especially in the rainfed and irrigated plots of the silty soil. The larger stress simulated by the Fe model in the rainfed and irrigated silty plots resulted in a smaller increase in biomass that was simulated in May by the Fe than by the Co model (Fig. 2a3a). The measurements of growth in the silty soil do not suggest that there was water stress in these plots in the silty soil indicating that the Co model better simulated transpiration and growth for these cases than the Fe model. Another way to test the RWU simulated by the different models is to compare the simulated soil water contents (Fig. 78). The Co and Fe models were able to simulate both dynamics and magnitude of SWC over-in different soil depths in-and for the different water treatments (average of RMSEs over all soil depths was 0.06 for both models, Appendix G). The Co and Fe models displayed lower water contents than the measured ones in the deeper layers at the late growing season (i.e. depth 80 and 120 cm) (Fig. 78). This could be due to the free drainage bottom boundary condition in the HILLFLOW water balance model, which implies that the water can only leave the soil profile but no water can flow in it. Capillary rise in the soil can keep the lower layers relatively wet (Vanderborght et al., 2010). In our simulation, the use of a soil depth of 1.5 m may not be deep enough to capture this effect. The simulated SWC were however very similar for both models. The larger RWU simulated by the Co than by the Fe model in the silty soil in May resulted in slightly lower simulated water contents by the Co model. But, the differences in simulated water contents by the two models were much smaller than the deviations from the observed water contents.

995 [Insert Fig. 7-8 here]

1000 For a few selected days, the diurnal course of T_{act} (or RWU), gross assimilation rate (Pg), stomatal conductance (gs), and leaf pressure head were measured. The measured and simulated data are shown in Fig. 89. Both Co and Fe models could mimic the daytime fluctuation of RWU and Pg in the sheltered plot of the stony soil, which is consistent with the adequate simulation of root growth (Fig. 34, F1P1) and SWC dynamics (Fig. 7a8c, F1P1). When the simulated ψ_{leaf} reached $\psi_{threshold} = -200$ m, the simulated RWU and Pg by the Co model showed a plateau (26 May in Fig. 8a9c, 8e9e, and 8e9j). The Co simulated better the

Formatted: Line spacing: 1.5 lines

Field Code Changed

010 diurnal courses of stomatal conductance as compared to the Fe, especially on a day with water stress-day (26 May, Fig. 9g and
9h). Using the leaf water pressure head threshold as an indication of water stress effects on stomata, Tuzet et al., (2003) and
Olmoso et al., (1996) also reported a considerable drop of P_g and transpiration. The sharp drop of simulated RWU and P_g which
is in contrast with measurement on the same day in the sheltered plot in silty soil illustrated that both models overestimated
the water stress. This related to the underestimation of both root growth (Fig. 34, F2P1) and SWC (Fig. 7b8d, F2P1) in the
1015 deeper soil layers by two models.

[Insert Fig. 8-9 here]

3.1.3 Whole plant hydraulic conductance from Couvreur RWU model

The Couvreur RWU model considers the root hydraulic conductance which relies on absolute root length. The root hydraulic
conductance is used to upscale to whole plant hydraulic conductance. The simulated K_{plants} reproduced the measured ones in
020 the different treatments quite well (Fig. 910). Our measured K_{plant} ranged from 1.5×10^{-5} to $10.2 \times 10^{-5} \text{ d}^{-1}$ (Fig. 910). These
values are in the same order of magnitude as values reported by Feddes and Raats, (2004) for ryegrass ranging from 6×10^{-5}
to $20 \times 10^{-5} \text{ d}^{-1}$. The simulated K_{plant} from our coupled root and shoot Co model followed the root growth and reached a
maximum at around anthesis. K_{plant} reduces toward the end of the growing season due to root death. For the sheltered plot of
the silty field, we would expect, based on the root density measurements (Fig. 34), the highest K_{plant} of all treatments. However,
025 this was not observed in the measurementsfield. Based on the measured total root lengths, we would also expect that K_{plant} of
the sheltered plot in the stony soilfield should be similar to K_{plant} in the other plots of the stony fieldsoil. But, K_{plant} was clearly
lower in the sheltered plot of the stony field-soil than in the other treatments in the stony fieldsoil. In the model simulations,
the lower K_{plant} in the sheltered plots compared to the other plots in the same fields-soil was due to a lower simulated total root
length. Since the differences in observed total root lengths were smaller (stony soil) or opposite (silty soil) to the differences
030 in simulated total root lengths, the smaller observed K_{plant} in the sheltered plots must have probably-other causes that are not
considered in the model. A potential candidate is the resistance to water flow from the soil to the root in the soil, which
increases considerably when the soil dries out, as was the case in the sheltered field plots.

[Insert Fig. 9-10 here]

The observed field data has been shown and compared with the simulated results from the two models in the above-mentioned
035 sections (3.1.1, 3.1.2, and 3.1.3). The data were collected for both crop growth (root, LAI, and biomass) and gas fluxes at
different scales (soil water flux and gas exchange from leaf to canopy) in two contrast soil types and under different water
treatments. To our knowledge, this is the unique experimental set-up and dataset for understanding soil-plant processes as well
as parameterizing and evaluating of soil-plant-atmospheric models. However, due to complex and costly construction of the
underground minirhizotrone facilities, there were no replicates for plots in our study. LAI and aboveground biomass showed
040 the large variability not only between water treatments but even in the same plot because of microclimate and soil
heterogeneities. The variability of tiller development also considerably influences stem-to-stem variability of sap flow. In
addition, the small size of plot did not allow having replicates for manual canopy chamber measurement because it might

1045 strongly disturb and alter crop growth, leaf gas exchange, and sap flow measurements of the surrounding areas. Nevertheless, despite of these shortcoming issues, the data illustrated the difference and variability among water regimes in two soil types, and over measured dates that it is still valid for modelling comparison and validation in this study.

3.2 Effects of changing root hydraulic conductance and leaf water pressure head thresholds

We conducted three sets of simulations. In the first set of simulations $K_{rs, normalized}$ was subjected to change. Fig. 40-11 illustrates the sensitivity of Co model to $K_{rs, normalized}$ in terms of above-ground biomass at harvest and cumulative RWU (from 15 March to harvest) for the different water treatments and soil types. For the rainfed and irrigated plots, an increase in $K_{rs, normalized}$ does not lead to a substantial increase in RWU and above ground biomass. This is a trivial consequence of the fact that water is not (irrigated plots) or only slightly (rainfed plots) limited in these cases. For the stony soil, a decrease of $K_{rs, normalized}$ by a certain factor leads to a stronger decrease in RWU and biomass than in the silty soil. This indicates that in the stony soil, less water is 'accessible' so that a decrease in root water uptake capacity by the crop has a stronger impact on RWU and biomass production than in the silty soil. For the sheltered plots, RWU and biomass production increases with $K_{rs, normalized}$ suggesting that increasing the water uptake capacity by the plants would increase the uptake and growth. But, increasing $K_{rs, normalized}$ by the same factor had a smaller relative effect on the RWU and biomass production than decreasing $K_{rs, normalized}$.

1055 [Insert Fig. 40-11 here]

Decreasing the specific weight of lateral and seminal roots increases the specific root length and thus total root length of root system, total root system hydraulic conductance, and thus and whole plant hydraulic conductance. However, for the considered range of specific weights, there was only a minor increase of above dry biomass and RWU (Fig. 40e11c-f). Reducing the specific root length by increasing the specific weights of lateral and seminal roots caused a stronger reduction in biomass and RWU, especially for the seminal root in the stony soil. High values of $\Psi_{threshold}$ led to more water stress and a sharp decrease in stomatal conductance and photosynthesis when Ψ_{leaf} was limited to its thresholds (Fig. 40g-11g & h). Our results suggested that $\Psi_{threshold}$ at -120 m or -140 m could overestimate the water stress while the $\Psi_{threshold}$ at -260 m could underestimate the stress.

1065 The impact of the change of the root segment conductance, specific weight of roots, and the leaf pressure head threshold at which stomata close on RWU and above ground biomass is amplified by the positive feedback between the above ground biomass, the root biomass, the total root length, the root system hydraulic conductance, and finally K_{plant} . Considering these interactions and feedbacks is important to evaluate the impact of changing a certain property of the crop on its performance in different soils and under different conditions.

1070 The root: shoot ratios of modern cultivars were lower than old wheat cultivars (Zhao et al., 2005; Siddique et al., 1990). However, the hydraulic conductance of single roots and the whole root system were increased in the modern cultivars and inversely correlated to the root: shoot ratio (Zhao et al., 2005). This indicates the water uptake ability of wheat roots was improved from wild to modern varieties during evolution with larger root system hydraulic conductance. In addition, recently, contrasting stomatal regulations were reported for different winter wheat genotypes that are related to the genotype specific

synthesis of ABA (Gallé et al., 2013). Plants with a high stomatal sensitivity to leaf water potential (pressure head) are then modelled with a higher reference (or critical) leaf water potential (-1.2 MPa) (or -120 m) while for species like wheat or lupine which are more tolerant to water stress a lower reference leaf water potential was used (i.e. -1.9 or -2.6 MPa) (equivalent to -190 m or -260 m, respectively) (Tuzet et al., 2003).

1080 The impact of changing root system properties or stomatal sensitivity to water ~~potential-pressure head~~ on root water uptake, stress, and crop growth cannot be assessed by a model that is not sensitive to these crop properties. Different to the Co model the Fe model is not sensitive to the total root length, the normalized root conductance, the specific root weight, and the leaf water ~~potential~~hydraulic head s at which stomata close. Therefore, the impact of introducing crop varieties with new properties cannot be assessed by this type of model. Only with the Co model the impact of the crop properties on growth and drought
1085 resilience can be studied.

4 Conclusion

~~We evaluated two different root water uptake modules of a coupled soil water balance and crop growth model. One root water uptake model was the often used Feddes model whereas the other, the Couvreur RWU model represents a “mechanistic” RWU model that explicitly simulates the continuum in water potential from soil to root, and to leaf based on the whole plant hydraulic conductance. The whole plant hydraulic conductance was calculated from the total root length and a root segment hydraulic conductance. All parameters of the model were derived from literature and from a previous study that was carried out at the same experimental site but for another growing season (Cai et al., 2018). Only one parameter of the Co model, i.e. a factor that was used to scale the root system conductance to the whole plant hydraulic conductance was manually adjusted. The soil, crop, and RWU parameters were applied to simulate crop biomass, LAI, root densities, and depth distributions, soil moisture contents, leaf water potentials, transpiration, and assimilation rates in two different soils and with each three different water treatments.~~

~~We evaluated two different root water uptake modules of a coupled soil water balance and crop growth model. One root water uptake model was the often used Feddes model whereas the other, the Couvreur RWU model represents a “mechanistic” RWU that explicitly simulates the continuum in water potential from soil to root, and to leaf based on the whole plant hydraulic conductance.~~ Overall, the measured biomass growth, LAI development, soil water contents, leaf water ~~potentials~~pressure
100 ~~heads,~~ and transpiration rates were well reproduced by both models. But, the Fe model incorrectly predicted more water stress and less growth in the silty soil than in the stony soil whereas the opposite was observed. ~~The Co model was able to predict the response of the crop to the different water stress conditions in the different soils and treatments. This was explained by more root growth in the silty soil which increased the root/plant hydraulic conductance, as was confirmed by direct estimates of the plant system conductances, and reduced the water stress. A mechanistic model that is based on plant hydraulics and links root system properties to RWU, water stress, and crop development can evaluate the impact of certain crop properties on crop performance in different environments and soils.~~
105 ~~The Fe model does not account for the higher plant conductance in the silty soil where more roots were simulated than in the stony soil. In addition, the Fe model does not consider root water uptake~~

compensation which reduces water stress. In other words, the Feddes approach did not possess the flexibility as compared to Couvreur model in simulating RWU for different soil and water conditions.

Based on the absolute root length, the Co model was able to simulate K_{plant} in different soils and treatments. The simulated K_{plant} followed the root growth and reached a maximum at around anthesis. However, the observed K_{plant} was lower in the sheltered plots although the observed total root lengths in these plots were almost similar (stony soil) or larger (silty soil) as compared to the irrigated and rainfed plots. Moreover, the higher simulated K_{plant} in comparison to the observed values in the sheltered plots suggested that the newly coupled model needs to consider the declined hydraulic conductance of the root-soil interface due to decreased soil water pressure head. The formation of air gaps at soil-root interface due to the root shrinkage of roots and root-soil contact loosening (Carminati et al., 2009) could induce a strong increase of hydraulic resistance to radial water flow between soil and roots.

A mechanistic model that is based on plant hydraulics and links root system properties to RWU, water stress, and crop development can evaluate the impact of certain crop properties (change of root segment conductance, specific weights of root, or leaf pressure head thresholds) on crop performance in different environments and soils. The Co model could capture the positive feedbacks between the aboveground biomass, the root length, the total root system hydraulic conductance, and finally K_{plant} .

Given the important role of root system properties for RWU and plant water stress, modelling root development and how it responds to water deficiency is crucial to predict the impact of water stress on crop growth. In this study, a higher total root length was simulated in the silty soil than in the stony soil because a higher specific root length was found for root growth in the silty soil. This can be considered as an extra relationship that requires attention in crop modelling. Crop growth models will need to consider soil specific calibration to account for differences in specific root length with soil. Alternatively, a more mechanistic description of root growth that predicts root specific length would reduce the amount of calibration in crop growth models. Another aspect in demand of improvement is the prediction of the root distributions with depth. In our simulations, highest root densities were simulated in the top soil whereas the observations showed higher densities in the deeper soil layers.

Examples of the detailed 3D root growth models that could improve the simulation of root distribution are given by Dunbabin et al., (2013). The coupling of a shoot model with the 3D root growth model that represents root system architecture simulated more accurate root distributions (at both top and subsoil layers) under drought conditions through a representation of root system architectures (Mboh et al., 2019). Nevertheless, simulating the third dimension of root growth would largely extend the parameter requirements which makes them more difficult for testing under the field. However, these observations were obtained from minirhizotubes and more validation with direct measurements of root distributions would be required. Finally, the model did not consider changes in carbon allocation to the root system that are triggered by stress. Therefore, the model simulated less roots in the water stressed sheltered plot of the silty soil whereas more roots were observed in this plot compared with the other plots in this soil. A more mechanistic description of the carbon allocation as a function of soil water conditions would be needed to refine the prediction of responses of root development to water stress.

Finally, the model did not consider changes in carbon allocation to the root system that are triggered by stress. Therefore, the model simulated less roots in the water stressed sheltered plot of the silty soil whereas more roots were observed in this plot compared with the other plots in this soil. A more mechanistic description of root: shoot partitioning of both carbon and nitrogen (Yin and Schapendonk, 2004) or carbon allocation as a function of soil water conditions (i.e. soil water potential in Kage et al., (2004) and Li et al., (1994)) would be needed to refine the prediction of responses of root development to water stress.

Future research should focus on testing the newly coupled model (~~HILLFLOW-Couvreur's RWU-SLIMROOT-LINTULCC2~~~~Couvreur~~ ~~HILLFLOW~~ ~~LINTULCC2~~) for other wheat genotypes and crop types (isohydric like maize) and for a wider range of soil and climate conditions. Further improvements should particularly be targeted leaf area simulation. Improving the modelling of leaf growth should result in better simulations of LAI and more accurate estimates of energy fluxes at canopy level.

Formatted: English (United Kingdom)

Appendices

Appendix A: Leaf photosynthesis and stomatal conductance calculation

$$AMAX_{l,t} = \frac{VCMAX_{l,t}(Ci_{l,t} - \Gamma^*)}{Ci_{l,t} + KMC \left(1 + \frac{O_2}{KMO}\right)} \text{fwat} \quad (\text{A1})$$

$$EFF_{l,t} = \frac{J}{2.14.5(Ci_{l,t} + 2\Gamma^*)} \quad (\text{A2})$$

$$FGR_{l,t} = AMAX_{l,t} \left(1 - e^{-I_{l,t} \frac{EFF_{l,t}}{AMAX_{l,t}}}\right) \quad (\text{A3})$$

$$Ci_{l,t} = Ca - \left(FGR_{l,t} \frac{1}{gs_{l,t}}\right) \quad (\text{A4})$$

$$gs_{l,t} = a_1 + \frac{b_1 FGR_{l,t}}{(Ci_{l,t} - \Gamma^*) \left(1 + \frac{DS_{l,t}}{D_0}\right)} \text{fwat} \quad (\text{A5})$$

AMAX is light saturated leaf photosynthesis ($\mu\text{M CO}_2 \text{ m}^{-2} \text{ s}^{-1}$); VCMAX is maximum carboxylation rate of Rubisco enzyme ($\mu\text{M m}^{-2} \text{ s}^{-1}$); Ci is intercellular CO₂ concentration ($\mu\text{M mol}^{-1}$); Ca is atmospheric CO₂ concentration ($\mu\text{M mol}^{-1}$); KMC is Michaelis-Menten constant for CO₂ ($\mu\text{M mol}^{-1}$); KMO is Michaelis-Menten constant for O₂ ($\mu\text{M mol}^{-1}$); O₂ is atmospheric oxygen concentration ($\mu\text{M mol}^{-1}$); Γ^* is CO₂ compensation point ($\mu\text{M mol}^{-1}$); EFF is quantum yield ($\mu\text{M CO}_2 \text{ MJ}^{-1}$); J is conversion energy from radiation to mole photon (mole photons MJ⁻¹); FGR is leaf photosynthesis rate ($\mu\text{M CO}_2 \text{ m}^{-2} \text{ s}^{-1}$); I is

the total absorbed flux of radiation ($\text{MJ m}^{-2} \text{s}^{-1}$); g_s is bulk stomatal conductance ($\text{mol m}^{-2} \text{s}^{-1}$); a_1 is residual stomatal conductance ($\text{mol m}^{-2} \text{s}^{-1}$) when $\text{FGR} = 0$; b_1 is fitting parameter (-); DS is the vapor pressure deficit at the leaf surface (Pa); D_0 is empirical coefficient reflecting the sensitivity of the stomata to VPD (Pa); l is sub-indices indicates canopy layer (sunlit and shaded leaf) (-); t is sub-indices indicates time of the day (-); fwat is water stress factor for stomatal conductance and maximum carboxylation rate (-);

Appendix B: Scale up leaf stomatal conductance to canopy resistance in hourly simulation

To scale up from leaf stomatal conductance to canopy and for computation efficiency, we approximate the integrals

$$\int_0^{LAI} f(l) dl$$

By Gaussian quadrature $LAI \sum_{j=1}^5 w_j * f(LAI * x_j)$ where x_j are the nodes and w_j the weights of the 5-point gaussian quadrature (Goudriaan and van Laar, 1994). LAI is the leaf area index and f is a function dependent on leaf area for instance $g_{\text{H}_2\text{O}}$.

The above mentioned bulk stomatal conductance to CO_2 ($g_{\text{S}_{\text{L}_t}}$ - $\text{mol m}^{-2} \text{s}^{-1}$) of sunlit and shaded leaf to stomatal conductance was converted to stomatal conductance to H_2O (m s^{-1}) based on the molar density of air.

$$g_{\text{SH}_2\text{O}_{\text{sun}}} = 1.56 * g_{\text{Sun}} / 41.66 \quad (\text{B1})$$

$$g_{\text{SH}_2\text{O}_{\text{shade}}} = 1.56 * g_{\text{shade}} / 41.66 \quad (\text{B2})$$

Leaf stomatal conductance to H_2O (m s^{-1}) was calculated based on fraction of sunlit leaf area FSLLA

$$g_{\text{SH}_2\text{O}_{\text{leaf}}} = g_{\text{SH}_2\text{O}_{\text{sun}}} * \text{FSLLA} + g_{\text{SH}_2\text{O}_{\text{shade}}} (1 - \text{FSLLA}) \quad (\text{B3})$$

~~Because the hourly weather input was used in hourly simulations (Feddes and Couveur), thus there was no Gaussian integration over time degree.~~ The hourly canopy conductance $\text{HourlyGSCropH}_2\text{O}$ (m s^{-1}) was calculated in Eq. (B4)

$$\text{HourlyGSCropH}_2\text{O} = LAI * \sum_{j=1}^5 w_j g_{\text{SH}_2\text{O}_{\text{leaf}}} \quad (\text{B4})$$

Hourly canopy resistance (s m^{-1}) was the reciprocal of hourly canopy conductance

$$\text{Hr}_s = 1 / \text{HourlyGSCropH}_2\text{O} \quad (\text{B5})$$

Hourly aerodynamic resistance (r_a) was calculated as Equation 4 in the Chapter 2 in the FAO Irrigation and Drainage Paper No. 56. (Allen et al., 1998). Assuming the leaf cuticle resistance and soil surface resistance were minor and neglected, the calculated canopy resistance (Hr_s) with $\text{fwat} = 1$ was directly used to calculate hourly crop evapotranspiration (ETP) hourly

185 using Penman-Monteith (Eq. B6) (See Equation 3, Chapter 2 in the FAO Irrigation and Drainage Paper No. 56, (Allen et al., (1998)).

$$ETP = \frac{\Delta(R_n - G) + \rho_a c_p \frac{(e_s - e_a)}{r_a}}{\lambda \left(\Delta + \gamma \left(1 + \frac{Hr_s}{r_a} \right) \right)} \quad (B6)$$

190 R_n is net radiation ($MJ\ m^{-2}\ h^{-1}$); G is soil heat flux ($MJ\ m^{-2}\ h^{-1}$); e_s is saturation vapor pressure at the air temperature (kPa); e_a is actual vapor pressure at the air temperature (kPa); ρ_a is mean air density at constant pressure ($kg\ m^{-3}$); c_p is the specific heat at constant pressure of the air ($1.013\ 10^{-3}\ MJ\ kg^{-1}\ ^\circ C^{-1}$); Δ is slope of the saturation vapor pressure-temperature relationship ($kPa\ ^\circ C^{-1}$); γ is the psychrometric constant of instrument ($kPa\ ^\circ C^{-1}$), Hr_s is ~~surface-canopy~~ resistance ($s\ m^{-1}$); r_a is the aerodynamic resistance ($s\ m^{-1}$); λ is the latent heat of vaporization ($2.45\ MJ\ kg^{-1}$).

Appendix C: Crop parameters used in the modelling work

Sub-models	Parameters	Explanation (unit)	Stony	Silty	Reference
LINTULCC2	VCMAX25	Maximum carboxylation rate of Rubisco at 25°C ($\mu M\ m^{-2}\ s^{-1}$)	62.1		Yin et al., (2009)
	Ca	Atmospheric CO ₂ concentration ($\mu M\ mol^{-1}$)	410		
	RGRL	Relative growth rate of leaf area during exponential growth ($^\circ C d^{-1}$)	0.007		van Laar et al., (1997)
	LAICR	Critical leaf area index (-)	5		van Laar et al., (1997)
SLIMROOT	RSROOT _{max}	Maximal elongation rate of seminal roots per day ($m\ d^{-1}$)	0.03		Watt et al., (2006)
	DRRATE	Daily fraction of dying roots (-)	0.008		
	RINPOP	Number of emerged plants per square meter (number m^{-2})	350		
	MAXDEP	Maximum root depth (m)	1.5		
	NRSP	Number of seminal root per plant (number plant ⁻¹)	3		Shorinola et al., (2019); Huang et al., (1991)
	WLROOT	Specific weight for lateral root ($g\ m^{-1}$)	0.0061	0.004	Jamieson and Ewert, (1999); Noordwijk and Brouwer (1991)
	WSROOT	Specific weight of seminal root ($g\ m^{-1}$)	0.02	0.015	Jamieson and Ewert, (1999); Huang et al., (1991)
Feddes	hlim1	Soil water potential-pressure head at anaerobic point limit (m)	0		Cai et al., (2018)
	hlim2	Upper limit of Soil water potential-pressure head range for optimal transpiration where optimum condition for transpiration (m)	-0.01		Cai et al., (2018)

Formatted Table

Formatted: English (United States)

hlim3h	Lower limit of Soil-water potential pressure head range for optimal transpiration for higher transpiration rate, T_{pot3h} (m)	-2.79	Cai et al., (2018)
hlim3l	Lower limit of Soil-water potential pressure head range for lower transpiration rate, T_{pot3l} (m)	-7.47	Cai et al., (2018)
hlim4	Soil water potential pressure head at wilting point (m)	-160	Cai et al., (2018)
T_{pot3h}	Higher transpiration rate (m d ⁻¹)	0.0048	Cai et al., (2018)
T_{pot3l}	Low transpiration rate (m d ⁻¹)	0.00096	Cai et al., (2018)
$\Psi_{threshold}$	Threshold of leaf water potential Critical leaf hydraulic head for specific plant (m)	-200	Cochard, (2002); Tardieu and Simonneau, (1998)
Couvreur	K_{rs} , normalized	Initial normalized root hydraulic conductance (cm d ⁻¹ /cm ²)	0.2544 10 ⁻⁵ Cai et al., (2018)
	K_{comp} , normalized	Initial normalized compensatory hydraulic conductance (cm d ⁻¹ /cm ²)	0.0636 10 ⁻⁵ Cai et al., (2018)
	β	Fraction to upscale from K_{rs} to K_{plant} (-)	0.55

Formatted: English (United States)

1195 Appendix D: Soil physical parameters at the top (0-30 cm) and subsoil (30-150 cm)

Soil types	Layers	α (m ⁻¹)	n (-)	l (-)	θ_r (m ³ m ⁻³)	θ_s (m ³ m ⁻³)	ks (m s ⁻¹)
Stony	Top soil	3.61	1.386	3.459	0.0430	0.3256	10.7*10 ⁻⁶
	Sub soil	4.95	1.534	3.459	0.0543	0.2286	5.83*10 ⁻⁸
Silty	Top soil	2.31	1.292	1.379	0.1392	0.4089	1.16*10 ⁻⁶
	Sub soil	0.50	1.192	1.379	0.1304	0.4119	1.73*10 ⁻⁶

The θ_r and θ_s are residual and saturation soil water content, respectively; α , n, l are empirical coefficients affecting the shape of the van Genuchten hydraulic functions ; ks is saturated hydraulic conductivity of the soil

Appendix E: Feddes root water uptake model

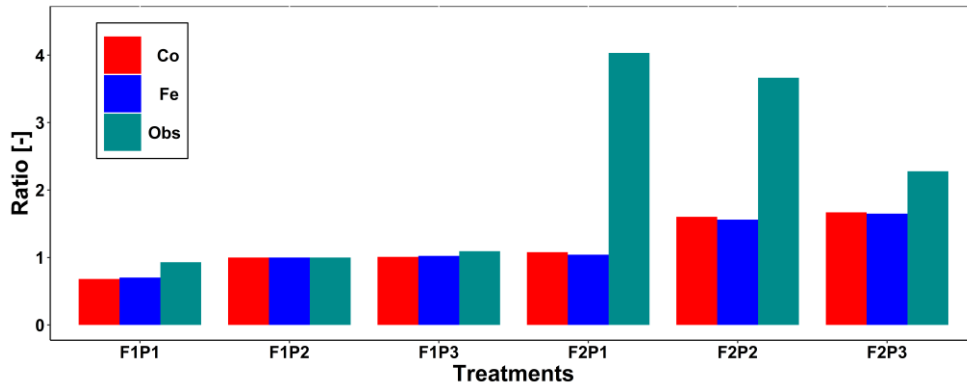
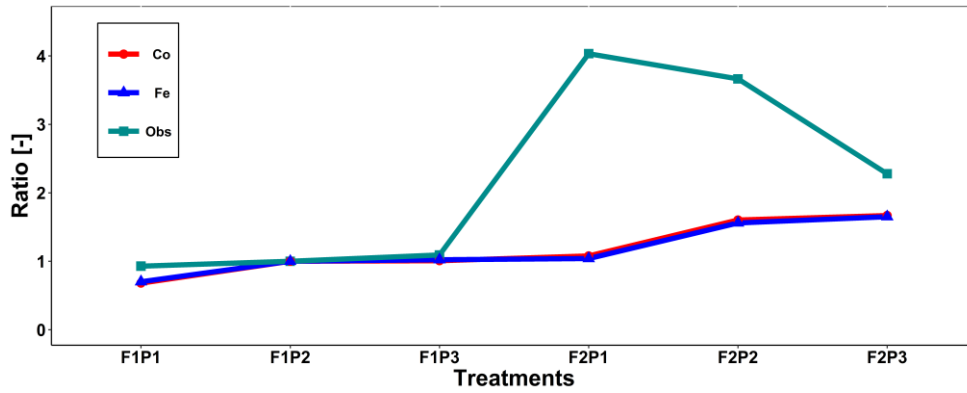
The root water uptake in HILLFLOW 1D model which is limited by soil water content in the root zone calculated by reduction of potential transpiration (T_{pot}). The semi-empirical reduction function $\alpha(\Psi_{m,i})$ is derived from ~~matrix potential~~soil pressure head (Feddes et al., 1978). The $\alpha(\Psi_{m,i})$ also depends on T_{pot} because ψ_3 (soil pressure head where optimum condition for transpiration) is calculated via piecewise linear function of T_{pot} (Wesseling and Brandyk, 1985). The root water uptake was calculated based on relative root length density which is output from the SLIMROOT root growth model.

$$\alpha(\Psi_{m,i}) = \begin{cases} 0 & \Psi_{m,i} \geq \psi_1, \Psi_{m,i} \leq \psi_4 \\ (\Psi_{m,i} - \psi_1)/(\psi_2 - \psi_1) & \psi_2 \leq \Psi_{m,i} \leq \psi_1 \\ 1 & \psi_3 \leq \Psi_{m,i} \leq \psi_2 \\ (\Psi_{m,i} - \psi_4)/\psi_3 - \psi_4 & \psi_4 \leq \Psi_{m,i} \leq \psi_3 \end{cases} \quad (F1)$$

$$\psi_3 = \begin{cases} \psi_{3h} & T_{pot} > T_{3h} \\ \psi_{3h} + \frac{(\psi_{3l} - \psi_{3h})(T_{3h} - T_{pot})}{(T_{3h} - T_{3l})} & T_{3l} < T_{pot} < T_{3h} \\ \psi_{3l} & T_{pot} < T_{3l} \end{cases} \quad (F2)$$

$\alpha(\Psi_{m,i})$ transpiration reduction as function of ~~matrix potential~~ soil pressure head (-); Ψ_1 is soil water pressure head at anaerobic limit (m); Ψ_2 is soil water potential at anaerobic point (m); Ψ_3 is soil pressure head water potential at wilting point (m); Ψ_4 is soil pressure head water potential at wilting point (m); Ψ_2 and Ψ_3 are upper and lower limits of pressure head for optimal transpiration (m), respectively soil water potential where optimum condition for transpiration (m); T_{pot} is potential transpiration (m d⁻¹); Ψ_{3h} is lower limit of pressure head range for optimal transpiration for high transpiration rate, T_{pot3h} (m); Ψ_{3l} is lower limit of pressure head range for low transpiration rate, T_{pot3l} (m); T_{3h} is higher potential transpiration rate (m d⁻¹); T_{3l} is lower potential transpiration rate (m d⁻¹).

Appendix F:



1215 Appendix F: Comparison -ratio of the observed total root length from minirhizotubes to observed total root length from F1P2 (green line with squares) and ratio of simulated total root length to the simulated total root length from F1P2 on 11 July 2016 (DOY 193) from Couvreur (Co, solid red, dots), and Feddes (Fe, solid blue, triangles) model at the sheltered (P1), rainfed (P2), and irrigated (P3) plots of the stony soil (F1) and the silty soil (F2)

1220

1225

Appendix G: Statistic RMSEs of soil water content simulated by the two models: the Couvreur (Co) and Feddes (Fe) in the sheltered (P1), rainfed (P2), and irrigated (P3) plots of the stony soil (F1), and the silty soil (F2). RMSE is $\text{cm}^3 \text{cm}^{-3}$

1230

	Depth (cm)	F1		F2	
		Co	Fe	Co	Fe
P1	10	0.09	0.09	0.08	0.08
	20	0.08	0.08	0.06	0.05
	40	0.04	0.04	0.07	0.07
	60	0.07	0.07	0.03	0.03
	80	0.08	0.08	0.03	0.03
	120	0.03	0.03	0.06	0.05
P2	10	0.10	0.10	0.09	0.08
	20	0.10	0.10	0.07	0.07
	40	0.06	0.06	0.07	0.06
	60	0.06	0.06	0.05	0.05
	80	0.05	0.04	0.06	0.06
	120	0.06	0.06	0.06	0.05
P3	10	0.11	0.12	0.10	0.11
	20	0.12	0.12	0.08	0.08
	40	0.08	0.08	0.09	0.08
	60	0.07	0.07	0.06	0.05
	80	0.05	0.06	0.06	0.06
	120	0.03	0.03	0.07	0.07

Data availability. The meteorological data were collected from a weather station in Selhausen (Germany) which belongs to TERENO network of terrestrial observatories. Weather data are freely available in TERENO data portal (<http://www.tereno.net>). The data which were obtained from the [minirhizotron](#) facilities (under and above ground) are available from the corresponding author on reasonable request and with permission from TR32 database (www.tr32db.uni-koeln.de).

Author contribution. TN, FW, ML, and JV conceived and designed the study. TN, HH, and ML collected the field data. TN performed modelling simulations and data analysis. TN wrote the paper. All authors read, commented, and revised the manuscripts.

Formatted: Font: Italic

Formatted: Font: Not Italic

1240

Competing interests. The authors declare that they have no conflict of interest

Acknowledgements. This research was financed by the German Science Foundation (DFG) within framework of Transregional Collaborative Research Center 32” Patterns in Soil-Vegetation-Atmosphere-Systems” (TR32, www.tr32.de). We thank Gunther Krauss for the technical support in modelling configurations. We thank our student assistants for their enthusiastic help for data collection in the field. We also thank Andrea Schnepf, Gaochao Cai, Miriam Zoerner, and Shehan Tharaka Morandage for providing soil water content, soil water potential, and root growth data.

1245

References

- Addiscott, T. M. and Whitmore, A. P.: Simulation of solute in soil leaching of differing permeabilities, *Soil Use Manag.*, 7(2), 94–102, 1991.
- 1250 Allen, R. G., Pereira, L. S., Raes, D. and Smith, M.: *FAO Irrigation and Drainage Paper - Crop Evapotranspiration.*, 1998.
- Bronstert, A. and Plate, E. J.: Modelling of runoff generation and soil moisture dynamics for hillslopes and micro-catchments, *J. Hydrol.*, 198(1–4), 177–195, doi:10.1016/S0022-1694(96)03306-9, 1997.
- Cai, G., Vanderborght, J., Klotzsche, A., van der Kruk, J., Neumann, J., Hermes, N. and Vereecken, H.: Construction of Minirhizotron Facilities for Investigating Root Zone Processes, *Vadose Zo. J.*, 15(9), 0, doi:10.2136/vzj2016.05.0043, 2016.
- 1255 Cai, G., Vanderborght, J., Couvreur, V., Mboh, C. M. and Vereecken, H.: Parameterization of Root Water Uptake Models Considering Dynamic Root Distributions and Water Uptake Compensation, *Vadose Zo. J.*, 0(0), 0, doi:10.2136/vzj2016.12.0125, 2017.
- Cai, G., Vanderborght, J., Langensiepen, M., Schnepf, A., Hüging, H. and Vereecken, H.: Root growth, water uptake, and sap flow of winter wheat in response to different soil water conditions, *Hydrol. Earth Syst. Sci.*, 22(4), 2449–2470, doi:10.5194/hess-22-2449-2018, 2018.
- 1260 Carminati, A., Vetterlein, D., Weller, U., Vogel, H.-J. and Oswald, S. E.: When Roots Lose Contact, *Vadose Zo. J.*, 8(3), 805–809, doi:10.2136/vzj2008.0147, 2009.
- Cochard, H.: Xylem embolism and drought-induced stomatal closure in maize, *Planta*, 215(3), 466–471, doi:10.1007/s00425-002-0766-9, 2002.
- 1265 Colombi, T., Kirchgessner, N., Walter, A. and Keller, T.: Root Tip Shape Governs Root Elongation Rate under, , 174(August), 2289–2301, doi:10.1104/pp.17.00357, 2017.
- Couvreur, V., Vanderborght, J. and Javaux, M.: A simple three-dimensional macroscopic root water uptake model based on the hydraulic architecture approach, *Hydrol. Earth Syst. Sci.*, 16(8), 2957–2971, doi:10.5194/hess-16-2957-2012, 2012a.
- 1270 Couvreur, V., Vanderborght, J. and Javaux, M.: A simple three-dimensional macroscopic root water uptake model based on the hydraulic architecture approach, *Hydrol. Earth Syst. Sci.*, 16, 2957–2971, doi:10.5194/hess-16-2957-2012, 2012b.
- Couvreur, V., Vanderborght, J., Beff, L. and Javaux, M.: Horizontal soil water potential heterogeneity: Simplifying approaches for crop water dynamics models, *Hydrol. Earth Syst. Sci.*, 18(5), 1723–1743, doi:10.5194/hess-18-1723-2014, 2014.
- van Dam, J. C.: Field-scale water flow and solute transport. SWAP model concepts, parameter estimation and case studies. [online] Available from: http://www.pearl.pesticidemodels.eu/pdf/swap_thesis.pdf, 2000.
- 1275 Desborough, C.: The impact of root weighting on the response of transpiration to moisture stress in land surface schemes, *Mon. Weather Rev.*, (1994), 1920–1930, doi:10.1175/1520-0493(1997)125<1920:TIORWO>2.0.CO;2, 1997.
- Dickinson, R. E., Henderson-Sellers, A., Rosenzweig, C. and Sellers, P. J.: Evapotranspiration models with canopy resistance for use in climate models, a review, *Agric. For. Meteorol.*, 54(2–4), 373–388, doi:10.1016/0168-1923(91)90014-H, 1991.
- Domec, J. and Prunyn, M. L.: Bole girdling affects metabolic properties and root , trunk and branch hydraulics of young

- 1280 ponderosa pine trees, *Tree Physiol.*, (28), 1493–1504, 2008.
- Dunbabin, V. M., Postma, J. A., Schnepf, A., Pagès, L., Javaux, M., Wu, L., Leitner, D., Chen, Y. L., Rengel, Z. and Diggle, A. J.: Modelling root-soil interactions using three-dimensional models of root growth, architecture and function, *Plant Soil*, 372(1–2), 93–124, doi:10.1007/s11104-013-1769-y, 2013.
- 1285 Egea, G., Verhoef, A. and Vidale, P. L.: Towards an improved and more flexible representation of water stress in coupled photosynthesis-stomatal conductance models, *Agric. For. Meteorol.*, 151(10), 1370–1384, doi:10.1016/j.agrformet.2011.05.019, 2011.
- Ewert, F., Rodriguez, D., Jamieson, P. D., Semenov, M. A., Mitchell, R. A. C., Goudriaan, J., Porter, J. R., Kimball, B. A., Pinter Jr., P. J., Manderscheid, R., Weigel, H. J., Fangmeier, A., Fereres, E. and Villalobos, F.: Effects of elevated CO₂ and drought on wheat: testing crop simulation models for different experimental and climatic conditions, *Agric. Ecosyst. Environ.*, 93(1–3), 249–266, 2002.
- 1290 Faria, R. T. De, Madramootoo, C. A., Boisvert, J. and Prasher, S. O.: Comparison of the versatile soil moisture budget and SWACROP models for a wheat crop in Brazil, *Can. Agric. Eng.*, 36(2), 57–68, 1994.
- Farquhar, G. D. and Caemmerer, S. Von: Modelling of Photosynthetic Response to Environmental Conditions, in *Physiological Plant Ecology II*, edited by O. L. Lange, pp. 550–582, Springer-Verlag Berlin Heidelberg., 1982.
- 1295 Feddes, R. A. and Raats, P. A. C.: Parameterizing the soil - water - plant root system, in *Wageningen Frontis Series*, vol. 6, pp. 95–141. [online] Available from: citeulike-article-id:4285297%5Cnhttp://209.85.173.132/search?q=cache:9fgslcr1dlgJ:library.wur.nl/frontis/unsaturated/04_feddes.pdf+Parameterizing+the+soil+?+water+?+plant+root+system&%5Cncd=1&%2338%5Cnhl=en&%2338%5Cnct=clnk&%2338%5Cngl=us&%2338%5Cnclnt=firef, 2004.
- 1300 Feddes, R. A., Kowalik, P. J. and Zaradny, H.: *Simulation of Field Water Use and Crop Yield*, Wiley. [online] Available from: https://books.google.de/books?id=zEJzQgAACAAJ, 1978.
- Feddes, R. A., Hoff, H., Bruen, M., Dawson, T., De Rosnay, P., Dirmeyer, P., Jackson, R. B., Kabat, P., Kleidon, A., Lilly, A. and Pitman, A. J.: Modeling root water uptake in hydrological and climate models, *Bull. Am. Meteorol. Soc.*, 82(12), 2797–2809, doi:10.1175/1520-0477(2001)082<2797:MRWUIH>2.3.CO;2, 2001.
- 1305 Gallardo, M., Eastham, J., Gregory, P. J. and Turner, N. C.: A comparison of plant hydraulic conductances in wheat and lupins, *J. Exp. Bot.*, 47(295), 233–239, doi:10.1093/jxb/47.2.233, 1996.
- Gayler, S., Ingwersen, J., Priesack, E., Wöhling, T., Wulfmeyer, V. and Streck, T.: Assessing the relevance of subsurface processes for the simulation of evapotranspiration and soil moisture dynamics with CLM3.5: Comparison with field data and crop model simulations, *Environ. Earth Sci.*, 69(2), 415–427, doi:10.1007/s12665-013-2309-z, 2013.
- 1310 van Genuchten, M. T.: A Closed-form Equation for Predicting the Hydraulic Conductivity of Unsaturated Soils, *Soil Sci. Soc. Am. J.*, 4, 892–898, 1980.
- ~~Goudriaan, J. and Van Laar, H. H. H.: *Modelling Potential Crop Growth Processes.*, 1994.~~
- Goudriaan, J. and van Laar, H. H.: *Modelling potential crop growth processes. Textbook with exercises.*, 1994.
- 1315 Henzler, T., Waterhouse, R. N., Smyth, a. J., Carvajal, M., Cooke, D. T., a.R., S., Steudle, E. and Clarkson, D. T.: Diurnal variations in hydraulic conductivity and root pressure can be correlated with the expression of putative aquaporins in the roots of *Lotus japonicus*, *Planta*, C(210), 50–60, 1999.
- Hernandez-ramirez, G., Lawrence-smith, E. J., Sinton, S. M., Schwen, A. and Brown, H. E.: Root Responses to Alterations in Macroporosity and Penetrability in a Silt Loam Soil, , doi:10.2136/sssaj2014.01.0005, 2014.
- Hsiao, T. C.: Plant responses to water stress, *Annu. Rev. Plant Physiol. Plant Mol. Biol.*, 24, 519–570, 1973.
- 1320 Huang, B. R., Taylor, H. M. and McMichael, B. L.: Growth and development of seminal and crown roots of wheat seedlings as affected by temperature, *Environ. Exp. Bot.*, 31(4), 471–477, doi:10.1016/0098-8472(91)90046-Q, 1991.
- Irmak, S. and Mutiibwa, D.: On the dynamics of canopy resistance : Generalized linear estimation and relationships with primary micrometeorological variables, *Water Resour. Res.*, 46, 1–20, doi:10.1029/2009WR008484, 2010.
- 1325 Jamieson, P. D. and Ewert, F.: The role of roots in controlling soil water extraction during drought : an analysis by simulation, *F. Crop. Res.*, 60, 267–280, 1999.

- Janott, M., Gayler, S., Gessler, A., Javaux, M., Klier, C. and Priesack, E.: A one-dimensional model of water flow in soil-plant systems based on plant architecture, *Plant Soil*, (341), 233–256, doi:10.1007/s11104-010-0639-0, 2011.
- Javot, H. and Maurel, C.: The role of aquaporins in root water uptake, *Ann. Bot.*, 90(3), 301–313, doi:10.1093/aob/mcf199, 2002.
- 1330 Jones, H. G.: *Plants and Microclimate: A Quantitative Approach to Environmental Plant Physiology*, Cambridge University Press. [online] Available from: <https://books.google.de/books?id=aPQ5WboKr1MC>, 1992.
- de Jong van Lier, Q., van Dam, J. C., Metselaar, K., de Jong, R. and Duijnisveld, W. H. M.: Macroscopic Root Water Uptake Distribution Using a Matric Flux Potential Approach All rights reserved. No part of this periodical may be reproduced or transmitted in any form or by any means, electronic or mechanical, including photocopying, recording, or , *Vadose Zo. J.*, 7(3), 1065–1078 [online] Available from: <http://dx.doi.org/10.2136/vzj2007.0083>, 2008.
- 1335 Kage, H., Kochler, M. and Stützel, H.: Root growth and dry matter partitioning of cauliflower under drought stress conditions: Measurement and simulation, *Eur. J. Agron.*, 20(4), 379–394, doi:10.1016/S1161-0301(03)00061-3, 2004.
- Katerji, N., Rana, G. and Fahed, S.: Parameterizing canopy resistance using mechanistic and semi-empirical estimates of hourly evapotranspiration : critical evaluation for irrigated crops in the Mediterranean, *Hydrol. Process.*, 129(August 2010), 117–129, doi:10.1002/hyp.7829, 2011.
- 1340 Kelliher, F. M., Leuning, R., Raupach, M. R. and Schulze, E. D.: Maximum conductances for evaporation from global vegetation types, *Agric. For. Meteorol.*, 73(1–2), 1–16, doi:10.1016/0168-1923(94)02178-M, 1995.
- Kramer, P. J. and Boyer, J. S.: *Water Relations of Plants and Soils*, Academic press, Inc. [online] Available from: <http://udspace.udel.edu/handle/19716/2830>, 1995.
- 1345 van Laar, H. H., Goudriaan, J. and Van Keulen, H.: SUCROS97 : Simulation of crop growth for potential and water-limited production situations., 1997.
- Langensiepen, M., Kupisch, M., Wijk, M. T. Van and Ewert, F.: Analyzing transient closed chamber effects on canopy gas exchange for optimizing flux calculation timing, *Agric. For. Meteorol.*, 164, 61–70, doi:10.1016/j.agrformet.2012.05.006, 2012.
- 1350 Langensiepen, M., Kupisch, M., Graf, A., Schmidt, M. and Ewert, F.: Improving the stem heat balance method for determining sap-flow in wheat, *Agric. For. Meteorol.*, 186, 34–42, doi:10.1016/j.agrformet.2013.11.007, 2014.
- Leuning, R.: A critical appraisal of a combined stomatal-photosynthesis model for C3 plants, *Plant Cell Environ.*, 18(4), 339–355, doi:10.1111/j.1365-3040.1995.tb00370.x, 1995.
- Li, X., Feng, Y. and Boersma, L.: Partition of photosynthates between shoot and root in spring wheat (*Triticum aestivu*, L.) as a function of soil water potential and root temperature, *Plant Soil*, (164), 43–50 [online] Available from: <https://link.springer.com/content/pdf/10.1007/BF00010109.pdf>, 1994.
- 1355 Lipiec, J., Siczek, A., Sochan, A. and Bieganski, A.: Geoderma Effect of sand grain shape on root and shoot growth of wheat seedlings, *Geoderma*, 265, 1–5, doi:10.1016/j.geoderma.2015.10.022, 2016.
- Mahfouf, J. F., Ciret, C., Ducharme, A., Irannejad, P., Noilhan, J., Shao, Y., Thornton, P., Xue, Y. and Yang, Z. L.: Analysis of transpiration results from the RICE and PILPS workshop, *Glob. Planet. Change*, 13(1–4), 73–88, doi:10.1016/0921-8181(95)00039-9, 1996.
- 1360 Maurel, C., Verdoucq, L., Luu, D.-T. and Santoni, V.: Plant Aquaporins: Membrane Channels with Multiple Integrated Functions, *Annu. Rev. Plant Biol.*, 59(1), 595–624, doi:10.1146/annurev.arplant.59.032607.092734, 2008.
- Mboh, C. M., Srivastava, A. K., Gaiser, T. and Ewert, F.: Including root architecture in a crop model improves predictions of spring wheat grain yield and above-ground biomass under water limitations, *J. Agron. Crop Sci.*, 205(2), 109–128, doi:10.1111/jac.12306, 2019.
- 1365 Merotto Jr, A. and Mundstock, C. M.: Wheat growth as affected by soil strength, *Rev. Bras. Ciênc. Solo*, 23(2), 197–202, 1999.
- Mo, X. and Liu, S.: Simulating evapotranspiration and photosynthesis of winter wheat over the growing season, *Agric. For. Meteorol.*, 109, 203–222, 2001.
- 1370 NOORDWIJK, M. V. A. N. and BROUWER, G.: Review of Quantitative Root Length Data in Agriculture, in *Plant Roots and*

- their Environment, vol. 24, edited by B. L. McMICHAEL and H. PERSSON, pp. 515–525, Elsevier., 1991.
- Olioso, A., Carlson, T. N. and Brisson, N.: Simulation of diurnal transpiration and photosynthesis of a water stressed soybean crop, *Agric. For. Meteorol.*, 81(1–2), 41–59, doi:10.1016/0168-1923(95)02297-X, 1996.
- 1375 Parent, B., Hachez, C., Redondo, E., Simonneau, T., Chaumont, F. and Tardieu, F.: Drought and Abscisic Acid Effects on Aquaporin Content Translate into Changes in Hydraulic Conductivity and Leaf Growth Rate: A Trans-Scale Approach, *Plant Physiol.*, 149(4), 2000–2012, doi:10.1104/pp.108.130682, 2009.
- Perez, P. J., Lecina, S., Castellvi, F., Mart, A. and Villalobos, F. J.: A simple parameterization of bulk canopy resistance from climatic variables for estimating hourly evapotranspiration, *Hydrol. Process.*, 532(December 2003), 515–532, doi:10.1002/hyp.5919, 2006.
- 1380 Peterson, C. A. and Steudle, E.: Lateral hydraulic conductivity of early metaxylem vessels in *Zea mays* L. roots, *Planta*, 189(2), 288–297, doi:10.1007/BF00195088, 1993.
- Prolingheuer, N., Scharnagl, B., Graf, A., Vereecken, H. and Herbst, M.: Spatial and seasonal variability of heterotrophic and autotrophic soil respiration in a winter wheat stand, *Biogeosciences Discuss*, 7, 9137–9173, doi:10.5194/bgd-7-9137-2010, 2010.
- 1385 Quijano, J. C. and Kumar, P.: Numerical simulations of hydraulic redistribution across climates: The role of the root hydraulic conductivities, *Water Resour. Res.*, 51(10), 8529–8550, doi:10.1002/2014WR016509, 2015.
- Rodríguez, D., Ewert, F., Goudriaan, J., Manderscheid, R., Burkart, S. and Weigel, H. J.: Modelling the response of wheat canopy assimilation to atmospheric CO₂ concentrations, *New Phytol.*, 150(2), 337–346, doi:10.1046/j.1469-8137.2001.00106.x, 2001.
- 1390 Saliendra, N., Sperry, J. and Comstock, J.: Influence of leaf water status on stomatal response to humidity, hydraulic conductance, and soil drought in *Betula occidentalis*, *Planta*, 196(2), 357–366, doi:10.1007/BF00201396, 1995.
- Shorinola, O., Kaye, R., Golan, G., Peleg, Z., Kepinski, S. and Uauy, C.: Genetic screening for mutants with altered seminal root numbers in hexaploid wheat using a high-throughput root phenotyping platform, *G3 Genes, Genomes, Genet.*, 9(9), 2799–2809, doi:10.1534/g3.119.400537, 2019.
- 1395 Sperry, J. S.: Hydraulic constraints on plant gas exchange, *Agric. For. Meteorol.*, 104(1), 13–23, doi:10.1016/S0168-1923(00)00144-1, 2000.
- Sperry, J. S., Stiller, V. and Hacke, U. G.: Xylem Hydraulics and the Soil–Plant–Atmosphere Continuum: Opportunities and Unresolved Issues, *Agron. J.*, 2003(95), 1362–1370, 1998.
- 1400 Srivastava, R. K., Panda, R. K., Chakraborty, A. and Halder, D.: Comparison of actual evapotranspiration of irrigated maize in a sub-humid region using four different canopy resistance based approaches, *Agric. Water Manag.*, 202(February), 156–165, doi:10.1016/j.agwat.2018.02.021, 2018.
- Stadler, A., Rudolph, S., Kupisch, M., Langensiepen, M., van der Kruk, J. and Ewert, F.: Quantifying the effects of soil variability on crop growth using apparent soil electrical conductivity measurements, *Eur. J. Agron.*, 64, 8–20, doi:10.1016/j.eja.2014.12.004, 2015.
- 1405 Tardieu, F. and Simonneau, T.: Variability among species of stomatal control under fluctuating soil water status and evaporative demand: modelling isohydric and anisohydric behaviours, *J. Exp. Bot.*, 49(March), 419–432, doi:10.1093/jxb/49.Special_Issue.419, 1998.
- Tardieu, F., Parent, B., Caldeira, C. F. and Welcker, C.: Genetic and Physiological Controls of Growth under Water Deficit, *Plant Physiol.*, 164(4), 1628–1635, doi:10.1104/pp.113.233353, 2014.
- 1410 Trillo, N. and Fernández, R. J.: Wheat plant hydraulic properties under prolonged experimental drought: Stronger decline in root-system conductance than in leaf area, *Plant Soil*, 277(1–2), 277–284, doi:10.1007/s11104-005-7493-5, 2005.
- Tsuda, M. and Tyree, M. T.: Whole-plant hydraulic resistance and vulnerability segmentation in *Acer saccharinum*, *Tree Physiol.*, (17), 351–357, 1997.
- 1415 Tuzet, A., Perrier, A. and Leuning, R.: A coupled model of stomatal conductance, photosynthesis, *Plant, Cell Environ.*, 26, 1097–1116, doi:10.1046/j.1365-3040.2003.01035.x, 2003.
- Vadez, V.: Root hydraulics: The forgotten side of roots in drought adaptation, *F. Crop. Res.*, 165, 15–24, 2014.

- Vanderborght, J., Graf, A., Steenpass, C., Scharnagl, B., Prolingheuer, N., Herbst, M., Franssen, H. H. and Vereecken, H.: Within-Field Variability of Bare Soil Evaporation Derived from Eddy Covariance Measurements, *Vadose Zo. J.*, 9, 943–954, doi:10.2136/vzj2009.0159, 2010.
- 1420 Vandoorme, B., Beff, L., Lutts, S. and Javaux, M.: Root Water Uptake Dynamics of various Under Water-Limited Conditions, *Vadose Zo. J.*, 11(3), 0, doi:10.2136/vzj2012.0005, 2012.
- Verhoef, A. and Egea, G.: Agricultural and Forest Meteorology Modeling plant transpiration under limited soil water : Comparison of different plant and soil hydraulic parameterizations and preliminary implications for their use in land surface models, *Agric. For. Meteorol.*, 191, 22–32, doi:10.1016/j.agrformet.2014.02.009, 2014.
- 1425 Vico, G. and Porporato, A.: Modelling C3 and C4 photosynthesis under water-stressed conditions, *Plant Soil*, 313(1–2), 187–203, doi:10.1007/s11104-008-9691-4, 2008.
- Wang, J., Yu, Q. and Lee, X.: Simulation of crop growth and energy and carbon dioxide fluxes at different time steps from hourly to daily, *Hydrol. Process.*, 21, 2267–2274, doi:DOI: 10.1002/hyp.6414, 2007.
- 1430 Watt, M., Silk, W. K. and Passioura, J. B.: Rates of Root and Organism Growth , Soil Conditions , and Temporal and Spatial Development of the Rhizosphere, *an*, 97, 839–855, doi:10.1093/aob/mcl028, 2006.
- Wesseling, J. G., Elbers, J. A., Kabat, P. and B. J. van den Broek: SWATRE: instructions for input, Internal Note, Winand Staring Centre, Wageningen, the Netherlands, , 1991, 1991.
- 1435 Wesseling, J. G. and Brandyk, T.: Introduction of occurrence of high groundwater levels and surface water storage in computer program SWATRE, , (1636), 1:48, 1985.
- Williams, J. and Izaurralde, R.: The APEX model, *Watershed Model.*, doi:10.1201/9781420037432.ch18, 2005.
- Willmott, C. J.: ON THE VALIDATION OF MODELS, *Phys. Geogr.*, 2(2), 184–194, doi:10.1080/02723646.1981.10642213, 1981.
- 1440 Wöhling, T., Gayler, S., Priesack, E., Ingwersen, J., Wizemann, H. D., Högy, P., Cuntz, M., Attinger, S., Wulfmeyer, V. and Streck, T.: Multiresponse, multiobjective calibration as a diagnostic tool to compare accuracy and structural limitations of five coupled soil-plant models and CLM3.5, *Water Resour. Res.*, 49(12), 8200–8221, doi:10.1002/2013WR014536, 2013.
- Yin, X. and Schapendonk, A. H. C. M.: Simulating the partitioning of biomass and nitrogen between roots and shoot in crop and grass plants, *NJAS - Wageningen J. Life Sci.*, 51(4), 407–426, doi:10.1016/S1573-5214(04)80005-8, 2004.
- 1445 Yin, X., Struik, P. C., Romero, P., Harbinson, J., Evers, J. B., Van Der Putten, P. E. L. and Vos, J.: Using combined measurements of gas exchange and chlorophyll fluorescence to estimate parameters of a biochemical C3 photosynthesis model: A critical appraisal and a new integrated approach applied to leaves in a wheat (*Triticum aestivum*) canopy, *Plant, Cell Environ.*, 32(5), 448–464, doi:10.1111/j.1365-3040.2009.01934.x, 2009.
- Zeng, X., Dai, Y.-J., Dickinson, R. E. and Shaikh, M.: The role of root distribution for climate simulation over land, *Geophys. Res. Lett.*, 25(24), 4533–4536, doi:10.1029/1998GL900216, 1998.
- 1450 Zhao, C., Deng, X., Shan, L., Steudle, E., Zhang, S. and Ye, Q.: Changes in Root Hydraulic Conductivity During Wheat Evolution, *J. Integr. Plant Biol.*, 47(3), 302–310, 2005.

1455

1460

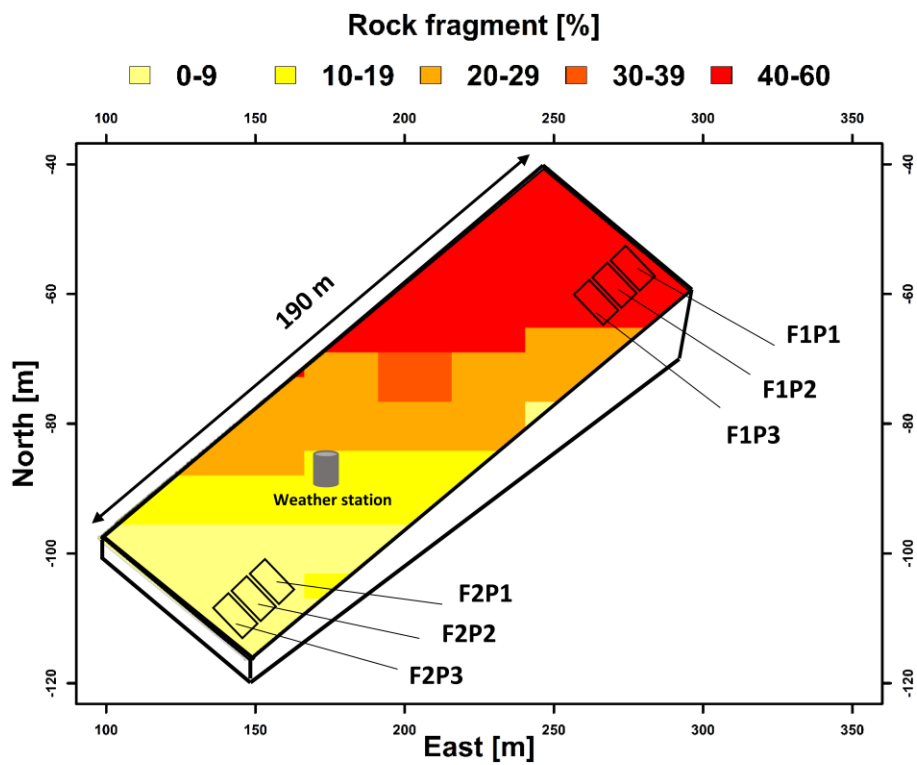


Figure 1: Description of the location of field experiment and set up of water treatments in the stony soil (F1) and silty soil (F2). P1, P2, and P3 are the sheltered, rainfed, and irrigated plots, respectively. Rock fragments are gravels with weathered granites.

1465

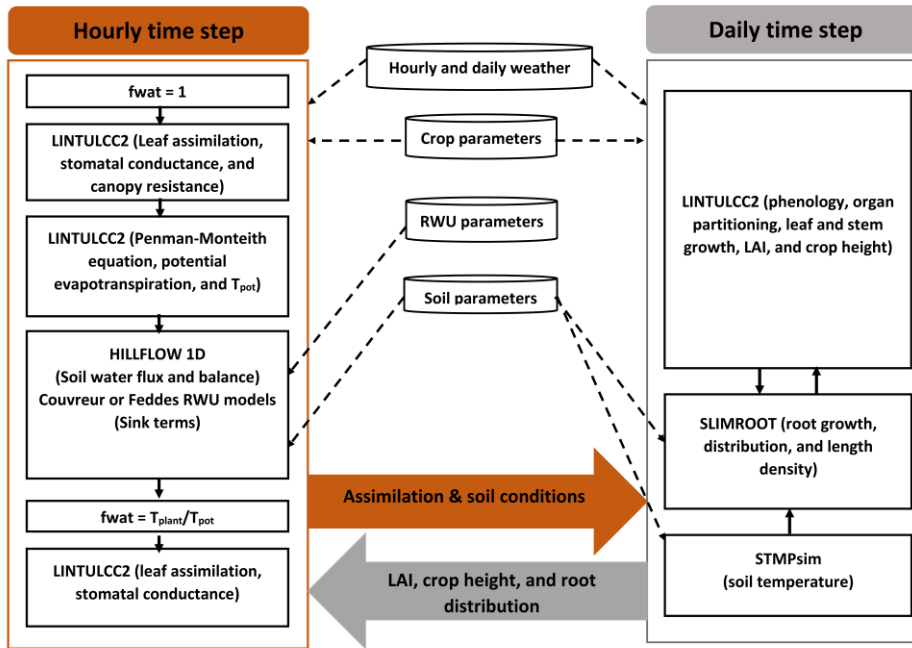


Figure 2: Description of the coupled root: shoot models in the study. The orange arrow indicates feedbacks from the hourly simulations to daily simulation while the grey arrow indicates feedbacks from the daily simulations to the hourly simulations. The dashed black arrows denote the weather input and parameters to the subroutines. The continuous black arrows indicate the links amongst the modelling subroutines.

Formatted: Font: 9 pt

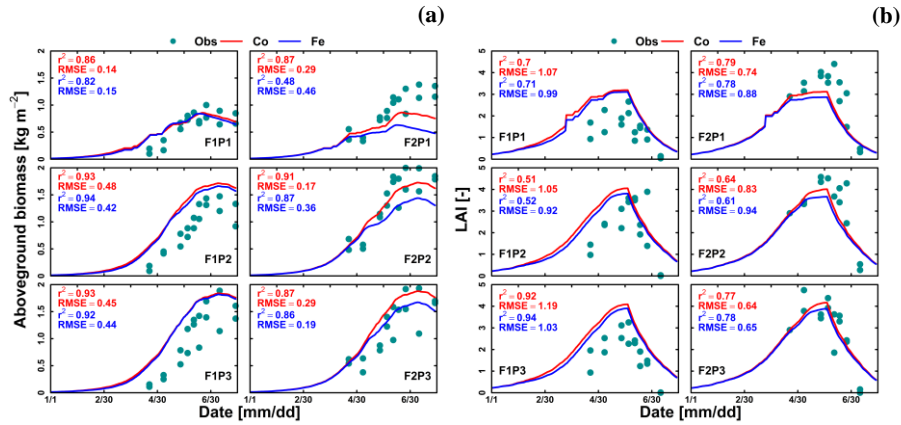


Figure 3: Comparison between observed (cyan dot) and simulated (a) above ground dry matter and (b) LAI by Couvreur (Co, solid red line), and Feddes (Fe, solid blue line) model at the sheltered (P1), rainfed (P2), and irrigated (P3) plots of the stony soil (F1) and the silty soil (F2). Note: crop germination was on 26th October 2015, data is shown here from 1 January to harvest 23 July 2016. RMSE in (a) is kg m⁻² while RMSE in (b) is unit less.

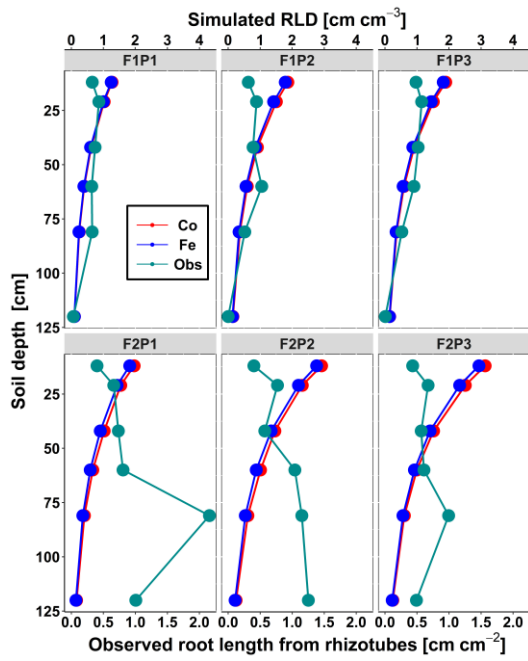


Figure 4: Comparison between observed root length from rhizotubes (cm cm^{-2}) (cyan line with dots) and simulated root length density (RLD) (cm cm^{-3}) from 10, 20, 40, 60, 80, and 120 cm soil depth at DOY 149 by Couvreur (Co, solid red) and Feddes (Fe, solid blue) model at the sheltered (P1) rainfed (P2), and irrigated (P3), of the stony soil (F1) and the silty soil (F2)

520

525

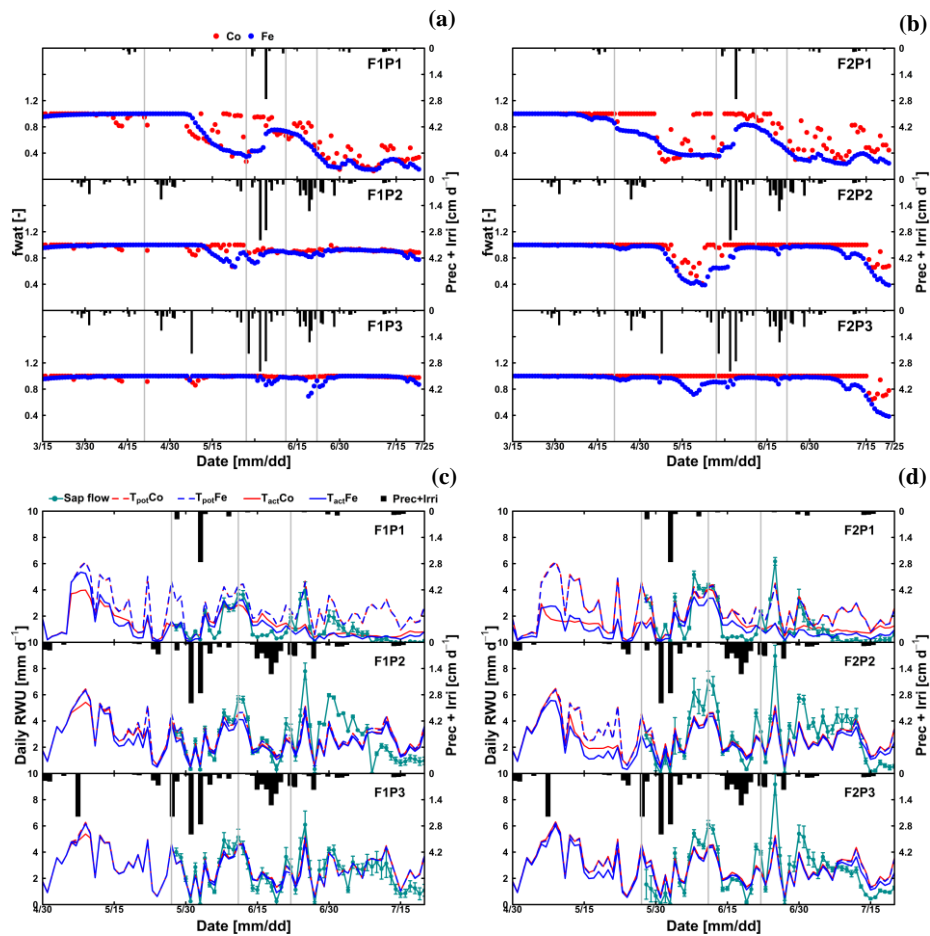
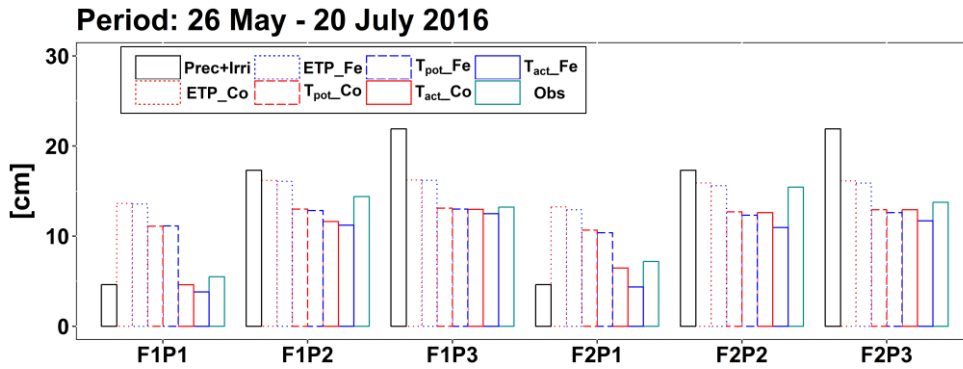


Figure 5: Daily transpiration reduction factor (fwat) (a, b) from 15 March to harvest 23 July 2016 and comparison between observed (cyan) and simulated root water uptake (RWU) and potential transpiration simulated (c, d) by Couvreur (Co, closed red), and Feddes (Fe, closed blue) from 30 April to 20 July 2016 model at the sheltered (P1), rainfed (P2), and irrigated (P3) plots of the stony soil (F1), and the silty soil (F2). Time series of precipitation (Prec) and irrigation (Irri) are given in the panels. Note: crop germination was on 26th October 2015.

1530

Vertical cyan bars represent the standard deviation of the flux measurements in the different stems. Vertical grey lines show days with the measured and simulated diurnal courses of root water uptake (RWU), leaf water pressure head (ψ_{leaf}), stomatal conductance (g_s), and gross assimilation rate (P_g) as used in Figure 9.

1535



1540 Figure 6. Cumulative precipitation and irrigation (Prec+Irri), potential evapotranspiration (ETP), potential transpiration (T_{pot}), actual
1545 transpiration (T_{act} or RWU) simulated by Couvreur (Co) and Feddes (Fe) model, and measured transpiration by sap flow sensors (Obs) from
1550 26 May to 20 July 2016 at the sheltered (P1), rainfed (P2), and irrigated (P3) plots of the stony soil (F1), and the silty soil (F2).
1555

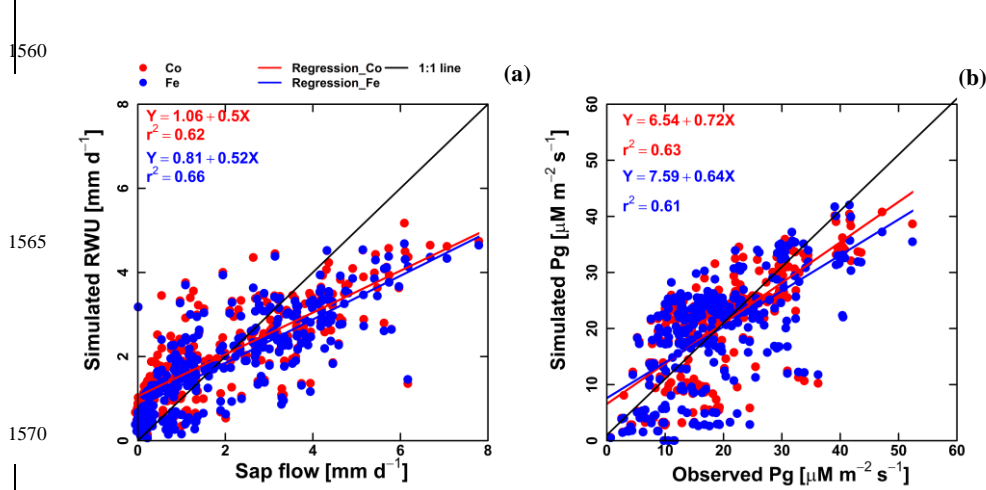


Figure 7. Correlation between observed and simulated (a) daily actual transpiration (or RWU) (b) hourly gross assimilation rate (Pg) from Couvreur (Co, red dot), and Feddes (Fe, blue dot) models of both fields (F1 and F2). Sap flow data was from 26 May until 20 July 2017 (n = 312). Gross assimilation rate from 08 measurement days (n = 302). RMSE in (a) is mm d^{-1} while RMSE in (b) is $\mu\text{M m}^{-2} \text{s}^{-1}$.

1575

1580

1585

1590

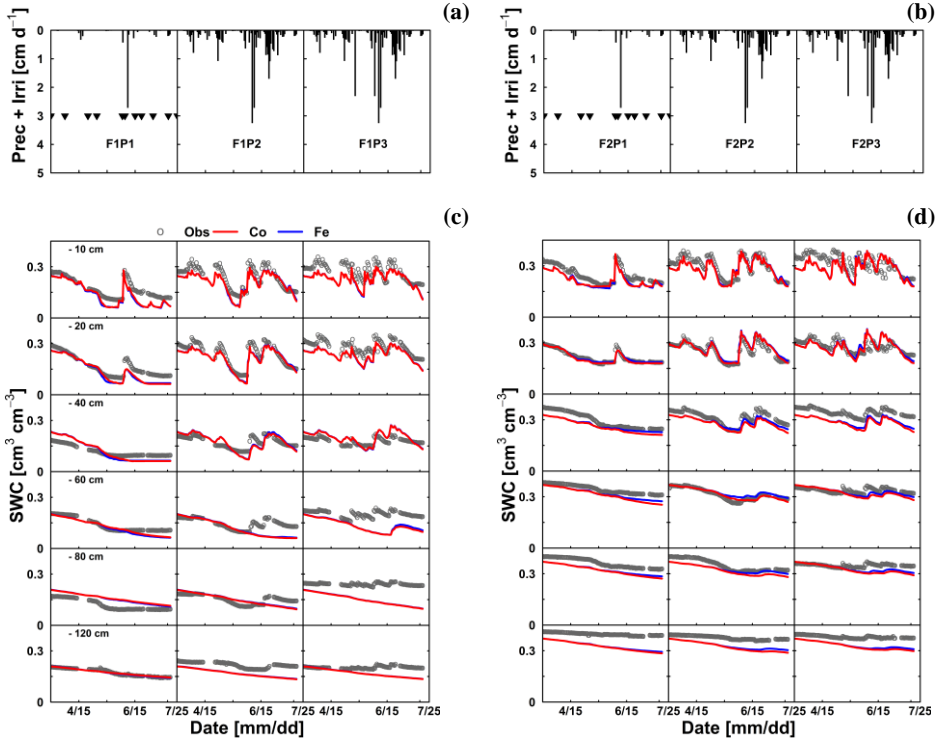
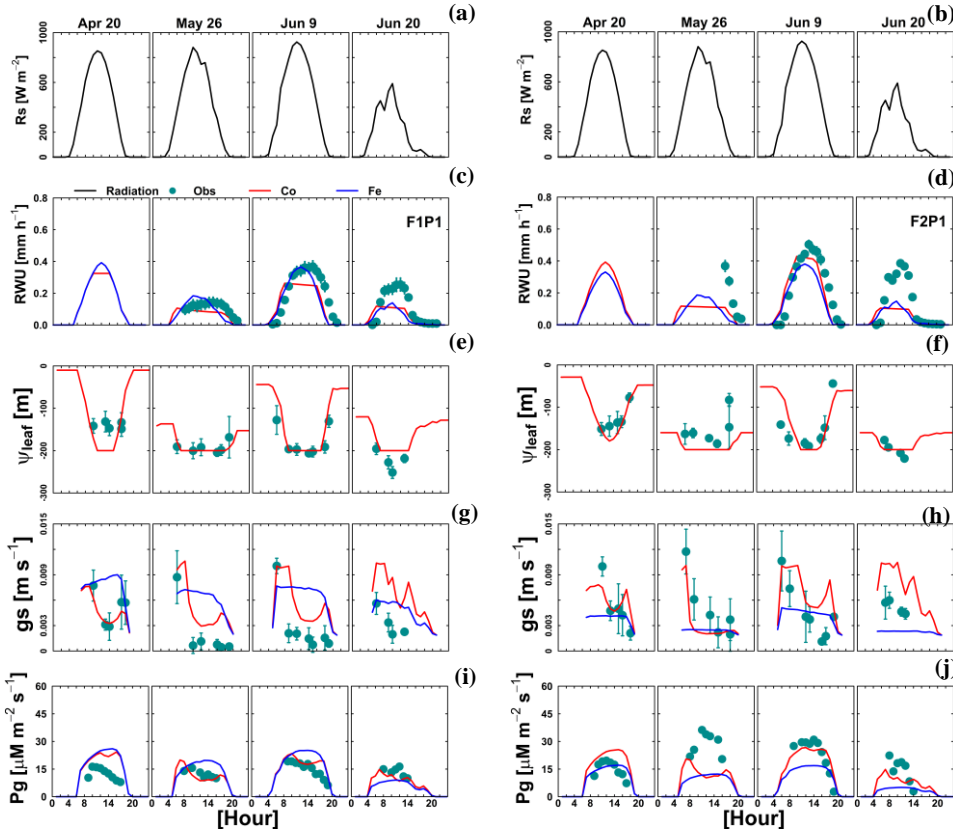


Figure 8: Illustrations of (a & b) time series of precipitation (Prec) and irrigation (Irr) and comparison between observed (black) and simulated soil water content (SWC) by the Couvreur (Co, solid red) and Feddes RWU model (Fe, solid blue) at six soil depths in at the sheltered (P1), rainfed (P2), and irrigated (P3) plots of (c) the stony soil (F1) (d) the silty soil (F2) from 15 March to 23 July 2016. Triangle symbols in the sheltered plots (F1P3 and F2P3) indicate the sheltered events.

595

600



1605 Figure 9: Diurnal courses of 4 selected measurement days: 20 April, 26 May, 9 June, and 20 June 2016 (a & b) global radiation (Rs) (c & d)
 1610 actual transpiration (RWU), (e & f) leaf water pressure head (ψ_{leaf}), (g & h) stomatal conductance to water vapor (gs), and (i & j) gross
 assimilation rate (Pg) at the sheltered plot (P1) of the stony soil (F1) and the silty soil (F2). The cyan, solid red, and solid blue dots denote
 the observed, simulated values from the Couvreur model (Co), and Feddes (Fe), respectively. Sap flow sensors were installed on 26 May
 2016 at 9 AM and 5 PM for F1P1 and F2P1, respectively. Simulated stomatal conductance are from sunlit leaves. The Feddes RWU model
 did not simulate leaf water pressure head.

1615

1620

1625

1630

1635

1640

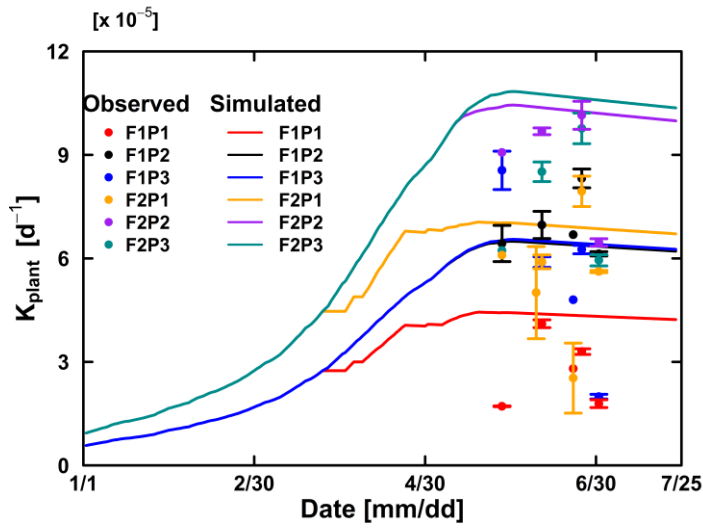
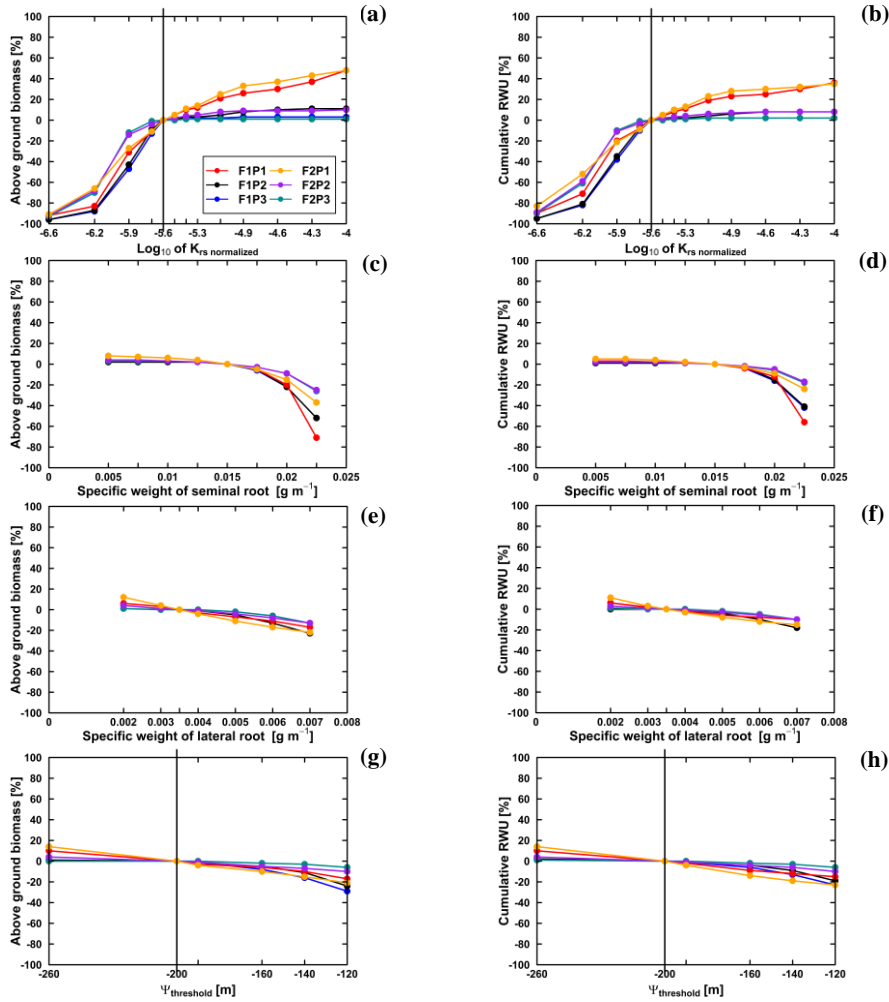


Figure 10: Comparison between observed (dot) and simulated plant hydraulic conductance (solid line) by the Couvreur (Co) model in the sheltered (P1), rainfed (P2), and irrigated (P3) plots of the stony soil (F1) and the silty soil (F2). The vertical bars represent the standard deviation of 6 hourly plant hydraulic conductance values at around midday (11 AM to 4 PM) in the measurement day. Note: crop germination was on 26th October 2015, data is showed here from 1 January 2016 to harvest 23 July 2016. Blue line was overlapped by the black line



670 Figure 11: Relative changes of simulated (Co model) above ground biomass at harvest (a, c, e, and g) and cumulative RWU (b, d, f, and h) (from 15 March to harvest 23 July 2016) with the changing $K_{rs, normalized}$, specific weights of seminal and lateral root, and leaf pressure head threshold ($\Psi_{threshold}$) in the sheltered (P1), rainfed (P2), and irrigated (P3) plots of the stony soil (F1) and the silty soil (F2). Vertical lines in (a) and (b) indicates the original value $K_{rs, normalized} = 0.2554 \cdot 10^{-5}$ (cm d⁻¹) while (g) and (h) indicates the $\Psi_{threshold} = -200$ m.

1675 Table 1: Quantitative and statistical measures of the comparison between two modelling approaches and the observed data for
 the 3 water treatments and 2 soil types. RMSE: root mean square error; r^2 : correlation coefficient; I: agreement index; n
 samples: number of sample. Couvreur RWU model (Co) and Feddes RWU model (Fe).

Variables	Statistical indexes	Co	Fe
Daily RWU (mm d ⁻¹)	RMSE	1.15	1.13
	r^2	0.62	0.66
	I	0.84	0.85
	n samples	312	312
Biomass (g m ⁻²)	RMSE	303	336
	r^2	0.91	0.86
	I	0.84	0.81
	n samples	54	54
LAI (-)	RMSE	0.92	0.90
	r^2	0.76	0.75
	I	0.77	0.77
	n samples	54	54
Gross assimilation rate ($\mu\text{M m}^{-2} \text{s}^{-1}$)	RMSE	6.34	7.26
	r^2	0.63	0.61
	I	0.86	0.83
	n samples	302	302

1680

1685